Investigations in Experimental Physics.

Collected Publications 1959 – 2002.

Ernest Hermann Hirsch
B.Sc.(Melb), M.Sc.(Adel).

This Thesis is presented for the degree of Doctor of Philosophy in the Faculty of Science, The University of Adelaide

2002.

Preface.

(a) General comments on the published scientific work presented for the Degree of Doctor of Philosophy.

The publications contained in this thesis deal with research carried out by me in the period from 1959 to 2002. This research was in the related areas of space charge phenomena, discharge physics, surface effects due to charged particle bombardment and thin film physics, together with associated questions in vacuum physics.

The majority of the investigations were made whilst I was working in the Electron Physics Group at W.R.E. (now D.S.T.O.) Salisbury SA, and I performed the remainder of the work as a Visiting Research Fellow in the Department of Physics and Mathematical Physics at the University of Adelaide.

(b) Statement concerning the authorship of the papers submitted.

Of the 34 papers submitted, 25 were published by me as the sole author. In the case of these 25 papers I produced the original ideas for the work, carried out the investigation and wrote the paper. For the remaining 9 papers, which each had one additional author, I initiated the research, took a major part in the experiments and wrote the paper. For these publications I would assess my contribution as follows:

Paper no.(32) was produced in collaboration with Dr J. Richards, another member of the Electron Physics Group. I consider my contribution to be 50%.

Papers nos. (33) and (34) were produced in collaboration with Mr. T.J. McKay, whose postgraduate research I was supervising in the Department of Physics and Mathematical Physics. My contribution was about 70%.

In the case of papers nos. (18),(19),(22),(23),(30) and(31) the co-authors were Messrs. T.R. Adams and I.K. Varga respectively, who were engaged as Technical Assistants in the Electron Physics Group. Their role was restricted to assisting me with the measurements. My contribution was about 90%.

List of publications submitted for the Degree of Doctor of Philosophy.

Section A. Anomalous energy distributions in thermionic emission systems

1. Anomalous energy distribution in electron beams.
E.H. Hirsch, J. Phys. D: Appl. Phys. **34**, 3229- 3233 (2001)

2. Abnormal electron temperatures and electron reflection in the cylindrical thermionic diode.
E.H. Hirsch, J. Phys. D: Appl. Phys.**35**, 2766-2771 (2002)

Section B. Excess energy electrons in magnetically confined electron clouds.

3. Excess energy electrons.
E.H. Hirsch, Brit. J. Appl. Phys. **15**, 909 –916 (1964)

4. On the mechanism of the Penning discharge.
E.H. Hirsch, Brit. J. Appl. Phys. **15,** 1535- 1543 (1964)

5. Auroral effects and excess energy electrons.
E.H. Hirsch, Nature **209**, 390 – 391 (1966)

6. The influence of thermionic emission velocities on the cut-off Characteristic of a cylindrical magnetron.
E.H. Hirsch, Int. J. Electronics **21**, 337-340 (1966)

7. Cut-off characteristics of a cylindrical magnetron.
E.H. Hirsch, Int. J. Electronics **21**, 521-533 (1966)

8. Modification of magnetron cut-off characteristics by the introduction of positive ions.
E.H. Hirsch, Int. J. Electronics **22**, 215-228 (1967)

9. Electron transport in the strongly cut-off magnetron.
E.H. Hirsch, Int. J. Electronics **22**, 297-305 (1967)

10. Reply to Comments on " Cut-off characteristics of a cylindrical magnetron.
E.H. Hirsch, Int. J. Electronics **22**, 591-594 (1967)

11. Space charge oscillations in the cylindrical magnetron.
E.H. Hirsch, Int. J. Electronics **23**, 497-509 (1967)

12 The concept of magnetic insulation.
E.H. Hirsch, Rev. Sci. Inst. **42**, 1371-1372 (1971)

Section C. Plasma physics.

13 The influence of probe potential on the electron energy distribution in a plasma.
E.H. Hirsch, J.Electr. and Control, **17**, 481- 489 (1964)

14. Plasma probes and the Langmuir paradox.
E.H. Hirsch, Int. J. Electronics **19**, 537-548 (1965)

15. Low pressure intermittend gas discharges.
E.H. Hirsch, Brit. J. Appl. Phys.**13**, 266-271 (1962)

Section D. Surface bombardment by charged particles.

16. Image formation by electron bombardment of metal targets.
E.H. Hirsch, Brit. J. Appl. Phys. **11**, 547-550 (1960)

17. The growth of carbonaceous contamination on surfaces undergoing ion bombardment.
E.H. Hirsch, J. Phys.D: Appl. Phys. **10**, 2069-2076 (1977)

18. Ion bombardment of materials containing alkali metal or alkaline earths.
E.H. Hirsch, and T.R. Adams, J.Phys. D: Appl.Phys. **12**, 1621-1632 (1979)

19. The action of water vapour on ion irradiated alkali silicate glasses.
E.H. Hirsch and T.R. Adams, Phys. Chem. Glasses, **21**, 120-127 (1980)

20. A new irradiation effect and its implications for the disposal of high level radioactive waste.
E.H. Hirsch, Science **209**, 1520-1522 (1980)

21. Stability of zeolites under electron irradiation.
E.H. Hirsch, Nature **293**, 759 (1981)

Section E. Thin film physics.

22. The effect of ion irradiation on the adherence of Germanium films.
E.H. Hirsch and I. K. Varga, Thin Solid Films, **52**, 445-452 (1978)

23. Thin film annealing by ion bombardment.
E.H.Hirsch and I.K. Varga, Thin Solid Films **69**, 99-105 (1980)

24. Stress in porous thin films through adsorption of polar molecules.
E.H. Hirsch, J.Phys. D: Appl. Phys. **13**, 2081-2094 (1980)

25. On the origin of adsorption stress in thin porous films.
E.H. Hirsch, J. Phys. D: Appl. Phys.**15**, 1991-1002 (1982)

Section F. Vacuum physics and associated techniques.

26. A precision pressure gauge for the range 0-30 mmHg.
E.H. Hirsch, J. Sci. Inst. **36**, 477 (1959)

27. Flow of gas through porous media in the region between molecular and viscous condition.
E.H. Hirsch, J.Appl. Phys. **32**, 977-982 (1961)

28. Vacuum measurements by means of alternating gas discharges.
E.H. Hirsch, Rev. Sci. Inst. **32**, 1373-1377 (1961)

29. Sputter ion pumps with thermionic electron injection.
E.H. Hirsch, J.Sci.Inst. **41**, 426-430 (1964)

30. Thermionic emission of positive ions from alkali tantalates.
E.H. Hirsch and I.K. Varga, J.Phys. D: Appl. Phys. **7**, 2355-2361 (1974)

31. Ion emission from a dispenser source with sodium silicate matrix.
E.H. Hirsch and I.K. Varga, Rev.Sci.Inst. **46**,338-339 (1975)

32. Pressure fluctuations in a diffusion pump using polyphenyl ether.
E.H. Hirsch and J. Richards, Vacuum **24**, 123-124 (1973)

33. A comparison of perfluoropolyether and silicone diffusion pump fluids.
E.H. Hirsch and T.J. McKay, Vacuum **43**, 301-304 (1992)

34. Emission and re-absorption of diffusion pump fluid breakdown products.
E.H. Hirsch and T.J. McKay, Vacuum **44**, 47-50 (1993)

Declaration.

The published papers presented in this thesis have not been submitted for a degree or diploma in any University, with the exception of paper no 3, material from which appeared in my M.Sc. thesis. I declare the statements I have made concerning the contributions of others to my papers to be true and accurate.

I consent to this thesis being made available for photocopying and loan if accepted for the award of the degree.

E. H. Hirsch

Summary of Section A.

Space charge effects in thermionic emission systems.

The research of this Section had its origin in a chance observation made in the course of some electron-optical measurements. It was noticed that a portion of the stray electrons which, after undergoing multiple scattering at the boundary walls, formed a background "atmosphere" within the apparatus, had energies higher than could be accounted for by the theoretically expected Maxwellian spectrum of emission velocities.

Paper no.1 aimed at finding the source of these unexpected energies. By varying the operating parameters of an apparatus that was in essence a thermionic diode, it was possible to rule out as a cause the Boersch effect, which is observed in high resolution electron microscopy as a broadening of the energy spectrum through stochastic electron-electron scattering. Instead it became apparent that the cause lay in an interaction of the electrons with space charge oscillations, located very close to the emitting surface.With temperature limited emission, i.e. with negligible space charge density, the energy spectrum was the normal Maxwell distribution expected for the particular emitter temperature. But when the degree of space charge limitation was raised to a level sufficient for oscillations to be sustained, the spectrum became non-Maxwellian and some electrons received "excess energy".

Since the conditions for the space charge interaction to occur was not critically dependent on the geometry of the emission system, it seemed likely that the effect should also have been present in previous work. A search of the literature revealed indeed accounts of abnormalities that seemed related to my observations,and these are reviewed in the paper.

These abnormalities were reported independently by several early observers working in the field of thermionic emission. These investigators were primarily concerned with measuring the "electron temperature" corresponding to what appeared to be Maxwellian distributions, and the temperature values obtained were often higher than expected, in some instances exceeding the melting point of all known materials. Some workers also observed a rise in electron temperature following the introduction of hydrogen, whilst other gases had no such effect.

Paper no.2 investigates further the reason for these abnormalities by firstly examining experimentally the suspected connection between the abnormally high reported electron temperatures and the non-Maxwellian distributions found in paper no.1.Secondly it seeks to elucidate the mechanism through which the introduction of hydrogen could influence the measured temperature.

The experiments were made with apparatus in its relevant aspects closely resembling that of the earlier workers. They showed that the abnormally high tempera-

tures were artifacts introduced by the measuring technique, which did not appropriately take into account space charge effects. Through these effects a Maxwell distribution was simulated where in reality none existed. The mechanism involved here is in fact closely allied to that leading to the Langmuir Paradox, which is more fully discussed in Section C.

Using a more appropriate method of measurement it was found that where the earlier method had yielded a Maxwell distribution, corresponding to an unduly high temperature, the actual energy distribution was non-Maxwellian and excess energy electrons were present.

It was also established that atomic hydrogen, formed at the hot emitter surface, was adsorbed at the boundary walls, where its presence caused increased reflection of electrons. As a result the space charge density in the emitter vicinity rose, affecting the oscillatory interaction with the electrons.

E.H. Hirsch (2001) Anomalous energy distribution in electron beams.
Journal of Physics D: Applied Physics, v. 34 (22), pp. 3229-3233, November 2001

E.H. Hirsch (2002) Abnormal electron temperatures and electron reflection in the cylindrical thermionic diode.
Journal of Physics D: Applied Physics, v. 35 (21), pp. 2766-2771, November 2002

Summary of Section B.

Space charge effects in magnetically confined electron clouds.

Paper no. 3 investigated experimentally the conditions under which excess energy electrons were produced in an electron cloud contained in a Penning type structure, consisting of a cylindrical anode with two negatively charged end plates, placed in an axial magnetic field. As distinct from the usual cold cathode discharge, the space charge density in this arrangement could be vastly increased by injecting thermionic electrons from an auxiliary hair pin filament, placed at the anode centre. Operation in ultra-high vacuum ensured that ionisation effects were negligible.

The experiments showed that the conditions for excess energy electron production were firstly that the space charge cloud was under radial confinement by the magnetic field, and secondly that the injected current was high enough to cause formation of a virtual cathode. Under these conditions a substantial number of excess energy electrons flowed against the applied negative potential to the end plates. Direct calorimetric measurements proved that as much as about 25% of the total energy introduced into the system could be diverted into this axial current flow. The dependence of the magnitude and energy distribution of the anomalous current flow on the operating parameters was determined.

In magnitude the excess energies observed in the magnetically confined clouds exceeded those found in the emission systems of section A by more than an order of magnitude, reaching values near 100 eV. As in section A, their distribution was non-Maxwellian, and of particular interest was the counter-intuitive result that whilst their number decreased exponentially, the most probable energy of the electrons impinging on a negative end plate increased as the potential of the electrode was made more negative.

Paper no. 4 is a study of processes in the cold cathode Penning discharge. Although Penning discharges had been known for a long time, and had been used extensively in vacuum measurements, their detailed mechanism was not well understood. The main purpose of the paper was to verify a model proposed by Knauer [(1)], according to which the discharge structure includes a thin electron sheath that undergoes $E \times B$ rotation very close to the anode surface. But as the investigation proceeded, it revealed other structural features of considerable complexity, that had not been previously observed.

According to Knaur's model, the electron impact ionisation, essential for the maintenance of the discharge in its normal mode, should occur primarily in the rotating electron sheath.

By observing the effect of inserting radially into the anode a large probe that could intercept electrons, it was established that there was indeed a thin critical sheath region close to the anode, where electron interception led to mode change in the discharge. The thickness of this critical region as well as the operating mode of the discharge varied with pressure, and following mode changes excess energy electrons appeared in different regions of the discharge.

In particular it was shown that in the regime of higher pressures finely structured streams of excess energy electrons issued from the sheath and impinged on the end plates. Their trajectory was at an angle to the axial magnetic field, but gas kinetic considerations precluded classical cross-field diffusion through molecular collisions as the dominant transport mechanism. It was therefore suggested that interaction with plasma oscillations that produced the excess energy electrons also led to their cross-field transport through the process suggested by Bohm et al. [2].

Paper no. 5 describes an experiment where thermionic electrons are injected into a confining magnetic mirror, and where excess energy electrons escape through the mirror ends. It points to the similarity between this effect and auroral phenomena, where electrons in the keV range leak from the outer radiation belt following the arrival of solar electrons with energies of about 100 eV, suggesting a similar acceleration mechanism may be involved in both cases.

Papers no. 6 to 11 are concerned with the cut-off problem in the cylindrical magnetron. This device consists of a cylindrical anode, equipped with end plates. It has a filamentary thermionic emitter on its axis, and is placed in an axial magnetic field. If one assumes zero electron emission velocity, an elementary theory predicts that, as the magnetic field strength is raised, the anode current should remain constant until a critical cut-off field B_c is reached, when the current should abruptly fall to zero. The cut-off problem consists in the observation that the actual onset of cut-off is more gradual, and the steepest part of the cut-off characteristic is frequently at field strengths a little below B_c. But more importantly, some anode current flows even at fields several times the critical value, and often the current decrease is non-monotonic.

The cut-off problem is not only one of intrinsic interest, but it has also a bearing on the development of the magnetic triode for the direct conversion of heat into electricity.

Paper no. 6 uses experimental data and the theory of Lindsay [3] to show that the cut-off broadening due to the distribution of electron emission velocities is too small to account for the observed features of the cut-off characteristics.

Paper no.7 examines in detail the dependence of the magnetron cut –off characteristics on the operating conditions. It is shown for the first time that beyond B_c

the axial distribution of the anode current is highly non-uniform and varies in a complex manner with the magnetic field strength. This axial variation of current density implies that the conventional two-dimensional treatment of electron motion in the magnetron cannot adequately describe the situation.
Although the cathode emission is highest at the anode centre, a major portion of the anomalous current impinges counter-intuitively on its ends. It is shown that current transport to the ends is only plausible by assuming motion under non-conservative forces, i.e.via the Bohm mechanism [2], through interaction with space charge oscillations. The occurrence of such interactions was confirmed by the appearance of excess energy electrons once the critical magnetic field strength had been reached.

The broadening of the cut-off characteristic by increasing the operating pressure was examined. The results show that at the low pressure otherwise used, cross-field electron diffusion through molecular impact played a negligible part, and that electron transport across the magnetic lines of force at cut-off was primarily through space charge interaction.

Paper no. 8. The conclusion of paper no.7, that electron transport at magnetic field strengths beyond cut-off was primarily due to space charge interactions, suggested the possibility of altering the cut-off characteristic of the magnetron through partially neutralising the space charge cloud by the introduction of positive ions. It was not possible to achieve such partial neutralisation by simply raising the pressure and relying on electron impact ionisation, since the implied electron-molecule collisions would themselves have contributed to the cross-field diffusion, and thus would have altered the cut-off curve. Instead caesium, the vapour pressure of which was sufficiently low to make collision effects negligible, was introduced into the system, and an adequate number of caesium ions could be produced by surface ionisation both on the filament and on appropriately placed heated platinum ribbons.

The experiment showed that modification of the characteristic through positive ion introduction was possible. Ions introduced in the cathode vicinity appeared most effective. Based on these experiments, together with earlier work on space charge distributions by Reverdin [4] and Twiss [5], it was conjectured that the anomalous anode current arose from a slipping stream interaction, probably located near the Hull radius. It was envisioned that here microscopic fluctuations, possibly originating in cathode vicinity, were amplified into macroscopic fluctuations.

In the course of the experiments it was also demonstrated for the first time that a small portion (approximately 1%) of the electrons reaches the anode of a magnetron with energies substantially above that corresponding to the anode potential. No violation of energy conservation is however involved, since other electrons arrive with correspondingly lower energy.

Paper no.9. Concurrently with my work, but not known to me at the time, Mouthaan and Suesskind [6][7] developed a theory for electron transport in the strongly cut off magnetron, where $B >> B_c$, on the hypothesis that there is an interaction with randomly varying space charge fields. The position of an electron is then a random function of time. On this basis they predicted an anode current variation according to $(V/B)^3$, where V is the anode potential, and they presented experimental data confirming this prediction.

Since a simple power law seemed difficult to reconcile with my own observations so far, I extended the experimental range to magnetic field strengths exceeding B_c by a factor 20, using both the apparatus of paper no.7 and commercial magnetrons of different geometry. In all cases the simple power law was not obeyed.

In trying to resolve the contradiction, I noted that Mouthaan [8] had derived the diffusion tensor describing the action of the randomly fluctuating fields in terms of random impulses, which each cause a displacement of the electron gyration centre by one gyration radius. The same model would equally well describe the action not of random fields, but of electron collisions with randomly moving gas molecules. The power law should therefore also apply to the classical electron cross field diffusion through molecular impact.

The dimensions of Mouthaan and Suesskind's apparatus were unusually large, and for technical reasons they were obliged to operate at pressures exceeding those in paper no7 by two orders. Both factors increase the collision probability during an electron trajectory, suggesting that Mouthaan and Suesskind's measurements may have been vitiated by the masking effect of gas collisions. Experiments confirmed this since, when in my experiments both pressure and anode potential were raised towards the values used by them, the power law was progressively approached.

Paper no 10 is a reply to comments by M.Bacal [9], who suggested that the results reported in paper no7, in particular the axial distribution of the anode current, might be caused by the voltage drop along the filament, together with an axial electron drift under the combined action of the applied radial electric field and the azimuthal magnetic field due to the heater current.

The paper discusses details of the electron motion and presents measurements, which show that the factors mentioned by Bacal cannot account for the observations.

Paper no. 11. The results of paper no.9 had shown that the space charge oscillations causing electron transport beyond cut-off were not random fluctuations, so

that as a corollary they had to follow a definite frequency pattern. A theory was therefore developed for an oscillatory process, based on the fact that at cut off there is a rotating electron cloud filling the anode volume. Velocity slip exists in this cloud, and with it the possibility for diocotron amplification to allow a disturbance in any narrow annular region to grow exponentially with distance. Particularly favourable conditions for growth exist if the annular circumference of the region is an integral multiple of the wavelength, so that " azimuthal resonance", i.e. a re-entrant wave pattern is obtained. The theory predicts that for thin cathodes and at low electron density this occurs at harmonics of the Lamor frequency. The frequency should therefore vary linearly with the magnetic field strength. This linear change should prevail even at higher electron density, when the plasma frequency introduces a correction to the Lamor value. Depending on operating conditions the wave growth could occur in one or more annular regions simultaneously.

Experiments made at low emission current confirmed these predictions. By capacitively coupling a sensitive receiver to one of the electrodes of the magnetron used in paper no 9, oscillations in the expected frequency range (order of 1000 Mc) were detected, and these frequencies correlated accurately with the appearance of sharp peaks in the cut-off characteristic.

From the measured values of the frequency, the theory allowed the electron density in the annular region concerned to be derived. This density varied by more than one order of magnitude within the rotating electron cloud, a fact compatible with the measurements of Reverdin[4],but not with the theory of Brillouin [10], which predicts a practically constant electron density.

At high emission current the frequency spectra became very complex, with evidence of oscillatory modes other that of azimuthal resonance being present.

Paper no 12 discusses a proposal by Winterberg [11] to construct a transformer for the gigavolt range, to be used for particle accelerators and other applications. To solve the insulation problem, this proposal envisaged firstly operation in ultrahigh vacuum to avoid the usual avalanche processes of gas breakdown. The remaining problem of vacuum breakdown through field emission at microscopic surface irregularities was to be eliminated through application of a suitably directed magnetic field, strong enough to ensure what is in effect magnetron cut-off.

My paper points out that, particularly since at field emission centres the current densities are extremely high, of order10^6 amp/cm^2, the space charge effects described in the previous papers of this section are liable to make cut-off incomplete. But even if there were complete cut-off, the return of field emitted electrons would merely ensure a zero net current, but would not suppress emission at the surface asperity. Here the current density would be very high and the temperature would rise locally. In a phenomenon well known in field emission research, sur-

face migration, enhanced by the higher temperature and the applied electric field, would cause the surface irregularity to grow. The consequent electric field intensification would in turn raise the emission current, and a run-away process would eventually lead to the evaporation of the emission centre and to vacuum breakdown.

The paper concludes that in principle not the application of a magnetic field, but only reduction of the surface electric field at the conductor could prevent vacuum breakdown.

References.

(1) Knauer W, J.appl. Phys.**33**,2093 (1962)
(2) Bohm D, Burhop E.H.S. and Massey H.S.W. "Characteristics of electrical discharges in magnetic fields" (New York McGraw-Hill (1949) p 64)
(3) Lindsay P J.Electron. Control **9,** 241 (1960)
(4) Reverdin D.L. J.appl. Phys. **22**, 257 (1951)
(5) Twiss R.Q. J. Electron. Control **1**, 1 (1955)
(6) Mouthaan K and Suesskind C . J. appl. Phys. **37**, 2598 (1966)
(7) Mouthaan K and Suesskind J Proc. IEEE **54**, 430 (1966)
(8) Mouthaan K Phys. of Fluids **8**, 1715 (1965)
(9) Bacal M Int. J. Electron. **22**, 591 (1967)
(10) Brillouin L Phys.Rev. **60**, 385 (1941)
(11) Winterberg F, Rev. Sci. Inst.

E.H. Hirsch (1964) Excess Energy Electrons.
British Journal of Applied Physics, v. 15 (8), pp. 909-916, August 1964

E.H. Hirsch (1964) On the Mechanism of Penning Discharge.
British Journal of Applied Physics, v. 15 (12), pp. 1535-1543, August 1964

E.H. Hirsch (1966) Auroral Effects and Excess Energy Electrons.
Nature, v. 209 (5021), pp. 390-391, January 1966

E.H. Hirsch (1966) The Influence of Thermionic Emission Velocities on the Cut-off Characteristic of a Cylindrical Magnetron.
International Journal of Electronics, v. 21 (4), pp. 337-340, 1966

E.H. Hirsch (1966) Cut-off Characteristics of a Cylindrical Magnetron.
International Journal of Electronics, v. 21 (6), pp. 521-533, 1966

E.H. Hirsch (1967) Modification of Magnetron Cut-off Characteristics by the Introduction of Positive Ions.
International Journal of Electronics, v. 22 (3), pp. 215-228, 1967

E.H. Hirsch (1967) Electron Transport in the Strongly Cut-off Magnetron.
International Journal of Electronics, v. 22 (4), pp. 297-305, 1967

E.H. Hirsch (1967) Reply to Comments on “Cut-off Characteristics of a Cylindrical Magnetron”.
International Journal of Electronics, v. 22 (6), pp. 591-594, 1967

E.H. Hirsch (1967) Space charge oscillations in the cylindrical magnetron.
International Journal of Electronics, v. 23 (6), pp. 497-509, 1967

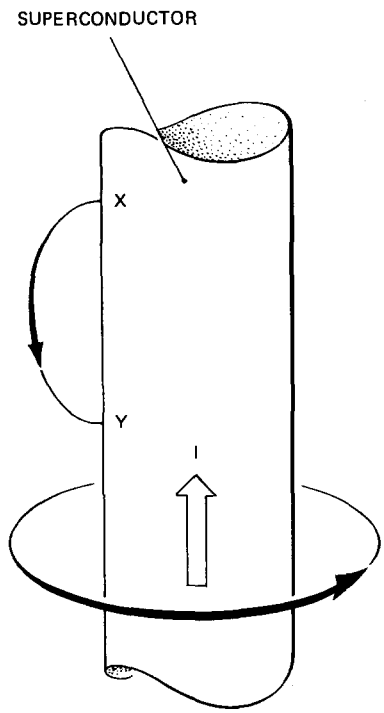

FIG. 1. Proposed use of magnetic field around a superconductor to suppress electron emission.

The Concept of Magnetic Insulation

E. H. HIRSCH
Weapons Research Establishment, Salisbury, South Australia
(Received 7 May 1971)

IN a recent paper Winterberg[1] has proposed the construction of a transformer for the gigavolt range, intended for applications such as the pumping of high power lasers and the production of high current fast particle beams for thermonuclear fusion research and high energy physics. It is the purpose of this note to draw attention to several points which seem to render the practicability of this proposal highly questionable.

The cardinal problem in constructing any device for operation at 10^9 V is clearly the prevention of insulation breakdown. Winterberg seeks to eliminate the usual gas avalanche processes by placing the windings into ultrahigh vacuum, which reduces the problem to one of preventing vacuum breakdown. An important factor here is electron field emission from microscopic surface irregularities, which at the high field strength envisaged will result in extremely high emission current densities, typically of the order of 10^6 A/cm^2 or more. To avoid breakdown due to this intense emission Winterberg proposes "magnetic insulation," an approach previously suggested by the same author[2] in a different context.

The basic idea is to suppress the emission by applying a suitably directed magnetic field of strength sufficient to force the electron orbits back onto the emitting surface, and it is proposed to derive this field from a current circulating in a superconductor (see Fig. 1). According to elementary theory, and for magnetic field strengths B exceeding a critical value B_c, an electron emitted at point X will describe a cycloid-like orbit in the azimuthal field, and will return to the emitter at point Y, resulting in zero net emission current.

One is concerned here with a form of magnetron cutoff. As numerous experiments have, however, established,[3–10] electron behavior under cutoff differs drastically from the predictions based on simple orbit calculations. Thus, although the anode current usually becomes considerably reduced at field strengths near the calculated critical value, cutoff is not complete, and significant anode current can flow at fields far exceeding B_c.

It has been demonstrated[10] that this anomalous electron behavior is due to space charge oscillations in the electron cloud which forms when $B \gtrsim B_c$. The electron motion in this cloud becomes nonconservative and a portion of the electrons receives a substantial amount of "excess energy."[11] Some of these excess energy electrons can, in fact, reach electrodes which are negative with respect to the emitter by amounts comparable to the total available anode potential. In the case of a gigavolt transformer, extremely high excess energies must therefore be expected.

Apart from the fact that anode current persists beyond cutoff, excess energy electrons issue forth from the cloud in various directions, some back-bombarding the cathode, while others stream axially in a general direction parallel to the emitting surface. Particularly under conditions of strong cutoff ($B \gg B_c$)[9] this axial stream can exceed the anode current by several orders of magnitude. Ultimately this stream will impinge on a boundary wall, where the high associated power dissipation is liable to lead to

breakdown, quite independently from the effects of the anode current. The cutoff anomaly therefore renders "magnetic insulation" impracticable in much the same way in which it has so far prevented the successful operation of magnetic triodes for direct energy conversion.[12,13]

But even if it should eventually prove feasible to stabilize the electron cloud to a sufficient degree, and thus to avoid violation of the cutoff criterion, magnetic insulation would still fail to present a solution to the problem of field-induced vacuum breakdown. As Fig. 1 shows, perfect cutoff would reduce the *net* emission current to zero, which however, does not imply that the individual surface irregularities would cease to emit at high intensity. The emission centers would still undergo Joule heating, leading ultimately to evaporation and vacuum breakdown. This well established process could only be accelerated by electrons returning from the vacuum to the emitter surface.

Clearly, the only way in which vacuum breakdown due to field emission from a given surface can be avoided is by reduction of the surface electric field.

[1] F. Winterberg, Rev. Sci. Instrum. **41**, 1756 (1970).
[2] F. Winterberg, Phys. Rev. **174**, 212 (1968).
[3] A. F. Harvey, *High Frequency Thermionic Tubes* (Wiley, London and New York, 1944).
[4] W. Fulop, J. Electron. Control **5**, 531 (1958).
[5] M. Bacal, J. Electron. Control **16**, 257 (1964).
[6] M. Bacal, J. Electron. Control **16**, 405 (1964).
[7] E. H. Hirsch, Int. J. Electron. **21**, 521 (1966).
[8] E. H. Hirsch, Int. J. Electron. **22**, 215 (1967).
[9] E. H. Hirsch, Int. J. Electron. **22**, 297 (1967).
[10] E. H. Hirsch, Int. J. Electron. **23**, 497 (1967).
[11] E. H. Hirsch, Brit. J. Appl. Phys. **15**, 909 (1964).
[12] G. F. Harris, G. D. Sims, and I. M. Stephenson, Electron. Technol. **39**, 27 (1962).
[13] M. Bacal and M. Teodorescu, Proc. ENEA-IEE, Thermionic Elec. Power Generation, London, 1965, Sec. II.

Detection of NO Impurity Particles in Plasmas Produced in Helium–Nitrogen Mixtures*

TILMANN D. MÄRK† AND H. J. OSKAM

Department of Electrical Engineering, University of Minnesota, Minneapolis, Minnesota 55455

(Received 17 May 1971)

DURING studies of the properties of decaying plasmas produced in nitrogen and rare gas–nitrogen mixtures it was found that the number densities of impurity ions and/or molecules had to be very small with respect to those of the ion and/or molecule studied in order to obtain reproducible data.[1,2] The main impurity ions were N_2H^+, NO^+, and NH^+, with the magnitude of their number density generally in that order. For most experimental conditions a relative NO^+ concentration less than 0.5% at 1 msec in the decay period was sufficient for a consistent interpretation and good reproducibility of the measurements.

A second method used for checking the purity consists of comparing the intensity of the NO-γ band emission with those of the Vegard–Kaplan bands and/or the second positive band emission.[3] No studies have been reported which compare the impurity detection sensitivities of the two methods. This communication relates to such a study.

The experimental system used is described in detail elsewhere.[2,4] The discharge region is a glass cylinder with metal end plates. One end plate is a perforated molybdenum electrode, while the other is made of Kovar metal and contains a small hole (60 μ diam and 40 μ length) through which the plasma ions effuse into the mass spectrometer. The mass spectrometer used is of the electric quadrupole type and the ions passing through the field analyzing region are detected by a 14-stage ion multiplier (RCA type C1787 K). The magnitude of the ion signal is measured by pulse counting techniques. The light emitted by the plasma is detected through the perforated molybdenum electrode and a quartz window by a monochromator (0.25 m Ebert) and associated detection equipment.

After a bakeout of the experimental tube and the gas handling system, helium purified by means of the cataphoretic segregation process[5] was mixed with nitrogen. The nitrogen concentrations used were 0.04 and 0.25%, and the total gas pressure was varied from 1.8 to 4.5 Torr. The discharge region was further cleaned by covering the discharge tube walls with a layer of molybdenum obtained by sputtering the molybdenum electrode.

For experimental conditions such that the NO^+ ion signal was less than $(0.3+0.1, -0.2)$% that of the dominant ion N_2^+, the ratios of the intensity of the (0,3) transition of the NO-γ band and those of the (4,1), (3,0) and the (4,2), (3,1), (2,0) transitions of the second positive bands were compared. The studies showed that the light intensity ratios were about two orders of magnitude larger than the ratio of the NO^+ and N_2^+ ion signals. This implies that the light detection method for revealing the presence of NO impurity molecules is by far more sensitive than the measurement of the relative concentration of NO^+ ions.[6]

* Work supported by the Air Force Cambridge Research Laboratories, Air Force System Command, under Contract No. AF19 (628)-4794 and by the National Science Foundation, under Grant No. GK-10395.

† On leave from the Institut für Atomphysik, Universität Innsbruck, A-6020 Innsbruck, Austria. The leave was made possible by a grant from the Max Kade Foundation, Inc., New York.

[1] R. E. Lund and H. J. Oskam, Z. Physik **219**, 131 (1969).
[2] T. D. Märk and H. J. Oskam (to be published).
[3] G. N. Hays and H. J. Oskam (to be published).
[4] G. F. Sauter, R. A. Gerber, and H. J. Oskam, Rev. Sci. Instrum. **37**, 572 (1966).
[5] R. Riesz and G. H. Dieke, J. Appl. Phys. **25**, 196 (1954).
[6] The intensity due to the (0,6) transition of the Vegard–Kaplan band was also compared with the intensity of the (0,3) transition of the NO-γ band for an NO^+ signal of 0.1% that of N_2^+. Even for this small NO^+ concentration, the Vegard–Kaplan transition was less than half as intense as the NO-γ transition.

Summary of Section C.

Plasma physics.

Paper no. 13 and paper no.14 are concerned with the resolution of the Langmuir Paradox, which arises from the fact that probe measurements in a hot cathode glow discharge indicate Maxwell distributions of electron energy even under conditions where losses to the boundary walls should make Maxwell distributions impossible. This situation throws some doubt on the validity of probe measurements as a means of measuring plasma electron energies.

The existence of boundary sheath oscillations, interaction with which Dracott [1] had proposed as being involved, proved very difficult to establish experimentally[2]. Therefore in this paper a sheath interaction is demonstrated by more indirect means. Measurements are made in a low pressure argon glow discharge by means of a flat probe, which at the same time acts as the entrance aperture of a cylindrical electrostatic energy analyser. In this way probe measurements could be compared with energy measurements on electrons that had passed through the probe sheath into a region outside the plasma.

The experiments showed that where the probe indicated a Maxwell distribution, the analyser data did not. Also varying the resonant properties of the probe sheath by changing the probe potential, modified drastically not only the number, but also the energy distribution of the electrons incident on the probe.

Paper no. 14 is a continuation of the investigation into the Langmuir Paradox by providing further evidence of sheath interaction. A number of probes of different geometry were placed together in a low pressure argon plasma. It was established that the electron temperatures indicated by these probes differed, as did the geometry dependent resonant properties of their respective plasma sheaths. The indicated temperatures therefore did not immediately reflect the mean electron energy in the bulk of the plasma.

In another set of experiments a "disturbing probe" was arranged opposite an "observing probe", facing it across the discharge vessel in such a way that electrons emerging from the disturbing probe sheath could reach the observing probe without undergoing a wall collision. Changing the negative potential of the disturbing probe altered the temperature seen by the observing probe. Similar changes were also caused by impressing a radio frequency signal on the disturbing probe, with the frequency in the range expected for plasma oscillations. But none of these changes were registered by several probes arranged so that they could not directly "see" the disturbing probe, i.e. they were inaccessible to electrons emerging from its sheath without intervening wall collisions.

These observations show clearly that it is possible for sheath interactions, and specifically for interactions with oscillations in the frequency range of plasma oscillations, to alter the electron temperature registered by a probe, without affecting the electron energy distribution in the plasma itself.

Paper no. 15 investigates the properties of an intermittent glow discharge, i.e. the properties of a discharge that performs relaxation oscillations when the discharge tube is fed from a voltage supply through a resistance and a shunt capacity C. A number of earlier investigators had shown that a plot of the relaxation period versus C intersected the abscissa at negative capacity values. This had led to ascribing a "self capacity" to the discharge, which Ritow [3] visualised as due to an "ionic condenser" formed by a layer of positive ions in front of the cathode. According to this picture field emission, due to the potential across this "condenser", played a significant part in the generation of charge carriers sustaining the discharge.

In an effort to examine the "ionic condenser" concept more closely, the structure and other characteristics of a glow discharge in air were studied in detail, using an electrode structure of cylindrical symmetry. Factors such as gas pressure and the parameters of the external circuit were taken into account.

Among other results it was found that the linear relationship between the relaxation period and the external capacity, on which the concept of self capacitance rested, is only approximate, and breaks down at sufficiently low capacity, where detailed measurement shows that the curve passes accurately through the origin. There is in fact no self capacity, and the earlier conclusion to the contrary was a consequence of neglecting the finite time required for the discharge to be extinguished between pulses.

The insights gained into the properties of the intermittent discharge eventually led to the development of a new vacuum gauge, described in paper no.28.

References.

(1) Dracott E.D. Thesis, University of London (1955)
(2) v. Gierke G. Ott W. and Schwirtzke F. Proc. 5th Int. Conf. on Ionisation Phenomena in Gases, Vol.2 1412 (1961)
(3) Ritow H, J. Electronics and Control 4, 11 (1958)

E.H. Hirsch (1964) The Influence of Probe Potential on the Electron Energy Distribution in a Plasma.
Journal of Electronics and Control, v. 17 (5), pp. 481-489, 1964

E.H. Hirsch (1965) Plasma Probes and the Langmuir Paradox.
International Journal of Electronics, v. 19 (6), pp. 537-548, 1965

E.H. Hirsch (1962) Low pressure intermittent gas discharges.
British Journal of Applied Physics, v. 13 (6), pp. 266-271, June 1962

Summary of Section D.

Surface bombardment by charged particles.

Paper no 16 arose from the need find a method for making visible the area on a metal target that had undergone weak electron bombardment, or to obtain the shape of an electron beam cross-section. This had to be possible when low particle energy or other circumstances prevented the use of fluorescent screens or photographic emulsions.

The method adopted relied on the fact that the background atmosphere of a conventional vacuum system contains a small component of hydrocarbon molecules, originating from back-diffused pumping fluid, O-rings and other sources. It was known from the work of Poole[1] that such hydrocarbons, when condensed on a surface undergoing electron irradiation, are dissociated into free radicals, that subsequently recombine into mechanically and chemically very stable polymers on the bombarded surface. The result of very prolonged bombardment is the build-up of a visible dark deposit.

Weak bombardment leaves no visible trace, but it was discovered that it affects the surface properties such that an image of the irradiated area can be obtained by attempting to deposit copper electrolytically on a bombarded metal target. It is found that the polymer partially inhibits the copper deposition.Under otherwise constant conditions the degree of inhibition increases with the length of the bombardment. Eventually saturation is reached, when no deposition at all occurs, although the polymer deposit still remains invisible.

Details of the process were studied and the influence of electron energy on the time required for saturation was determined. It was found that the process could be used with electron energies as low as 5 eV.

Australian Provisional Patent Specification No. 18837/53 lists among possible applications of the process the production of patterns, ornamental effects, shallow grooves or recesses on a surface. It therefore in principle foreshadows what, with the subsequent advent of integrated circuits, became known as electron lithography.

Paper no 17 is concerned with the growth of carbonaceous deposits formed from adsorbed hydrocarbon molecules through bombardment not by electrons, as in paper no.16, but by positive ions. This process had not been systematically studied before, although it is of obvious technological importance in connection with ion deposition of materials, ion implantation and surface treatment by ion etching.

My own observations had shown that the deposit thickness was not a monotonic function of the bombardment intensity. Under typical conditions no deposit was seen on the target in the area of intense irradiation within the beam core. But as the beam edge was approached, a sharply demarcated thick film became visible, which eventually became thinner further out from the beam centre.

Equations were derived for the growth dynamics of the contamination deposit, taking into account factors such as the arrival rates of hydrocarbons and ions, the cross-sections for re-evaporation, ion desorption, dissociation and polymerisation of the hydrocarbons, as well as the projected range of ions in the polymer. It was shown that the non-monotonic growth rate of the deposit was the result of the interplay of these various factors.

Although numerical values for some of the cross-sections were not well known, the analysis allowed some practical conclusions to be drawn. Under typical vacuum conditions the equilibrium surface coverage by hydrocarbons is about 1 monolayer. Provided the ion energy is sufficient (1-3 keV) to give a sputtering yield of at least 0.5 to 1 atom/ion, the polymer layer formed will have a thickness of about 1/J monolayers, where J is the ion current density in μ amp/cm^2.

This shows that readily achievable ion current densities are sufficient to make the degree of contamination small. But near the beam edge, where the density drops, a substantial deposit will unavoidably form if the bombardment time is long enough. Therefore in appropriate cases beam scanning should be used, to ensure that the effective beam edge does not lie in a target region where contamination build-up must be avoided.

Paper no 18, together with the succeeding papers nos.19,20 and 21, are concerned with a new irradiation effect. Although this effect was observed in certain materials following irradiation by either positive ions, electrons in the keV range or Cu - Kα radiation, it was only studied in detail with positive argon ions.

The effect was first noticed during an attempt to ion-polish potassium dihydrogen phosphate (KDP), an electro-optic material used in laser systems. Since this material is fairly soft, it is practically unavoidable that small particles of any conventional polishing agent remain embedded in its surface. At high laser power levels surface damage can develop at such impurities, either through selective absorption of radiation or through field emission caused by local intensification of the electric field.

Ion polishing seemed to offer a possibility for avoiding this difficulty, but when a KDP specimen, bombarded with 1 keV argon ions, was removed from the vacuum system, a reaction set in, which caused its surface to be severely corroded within a few minutes. It was established that water vapour was the only atmospheric constituent necessary for this to occur.

The effect was studied in detail, and a mechanism that embraces all the observed experimental facets was proposed. It may be summarised as follows:
Ions incident on material MX detach cations M^+ from their normal position according to

$$MX + \text{ion irradiation} \rightarrow M^+ + X^- \qquad (1)$$

They also create catalytically active surface sites to where the cations can migrate and be converted through electron transfer from M^+ to M.

In the presence of H_2O

$$M + H_2O \rightarrow MOH + H\uparrow \qquad (2)$$

and

$$X^- + H_2O \rightarrow XH + OH^- \qquad (3)$$

At suitable surface sites the hydroxyl produced in step (3) can break the M-X bond so that

$$MX + OH^- \rightarrow MOH + X^- \qquad (4)$$

Even long after the irradiation has ceased, provided water vapour is available steps (3) and (4) can be cyclically repeated indefinitely, with further accumulation of the water soluble product MOH, which is found to be only loosely attached to the surface.

This reaction scheme should be applicable, albeit with different reaction rates, to all materials containing alkali metals or alkaline earths. This was indeed confirmed for a wide range of materials, but the reaction rate was particularly fast in KDP. On the other hand alkali free single crystals of sugar and urea did not show the effect, which gave further credence to the proposed reaction scheme.

Paper no 19 investigates in detail the new radiation effect in ion- irradiated silicate glasses. Whilst in crystalline materials the primary reaction, leading to hydrogen evolution, was apparent typically within about one minute, it took between several hours and several months after irradiation before signs of the reaction could be detected in glasses. Since surface migration of reactants is involved in the process, it is not surprising that a moderate temperature rise increased the reaction rate. Also, as expected, the rate was more rapid in materials with higher alkali content, and no reaction was detected in alkali free fused silica.

In crystalline materials the catalytically active sites had been found mainly in regions such as crystallographic ledges, where dangling bonds are available. In amorphous substances the place of such sites is taken by compositional discontinuities, such as exist at the boundary of micron-sized minority phase particles

within the main matrix. The corrosion reaction then propagates from the boundary throughout the minority phase, and the corrosion product becomes visible under the microscope as a small spot. As the product is highly water soluble, such spots are readily washed off.

Electron microscopic examination of the orientation of corrosion centres revealed patterns of long range order not expected in amorphous materials. These appear to reflect the pattern of flow of the main matrix material around the minority phases during the working of the glass.

Paper no 20 discusses the possible implications of the new irradiation effect, described in papers no.18 and 19, for the long term immobilisation of high level nuclear waste in glass-like storage matrix materials. Since ^{90}Sr and ^{137}Cs are among the fission products that need to be stored, the alkali metal content required for the effect to occur is assured. In amorphous materials the effect had been shown to start at phase boundaries, and in the multiconstituent glasses proposed for waste immobilisation, phase separation is known to be very pronounced [2][3][4]. Important amongst these phases are particularly the molybdates, which arise from the reaction of the fission product Mo with the alkali isotopes present. One would expect conversion of these materials into water soluble products to cause an increase in the leach rate of radioactivity from the storage matrix, particularly since one molybdate, $CaMoO_4$, had already been shown in paper no.18 to be susceptible to attack. The paper draws attention to a number of aspects which need further clarification before the relevance of the effect for nuclear waste storage can be fully assessed.

Paper no. 21 discusses the degradation of zeolites during electron microscopic examination, reported by Bursill et al. [5][6]. These authors explain the observed structural change in the material by the production of OH^- through electron impact. The hydroxyl is considered to weaken the bonds in the aluminosilicate framework, causing it eventually to collapse.

In the paper I point to our irradiation effect, and suggest that the action of the electron beam might rather be the detachment of cations from their normal position, and the creation of catalytically active sites, where electron transfer to the cations can take place.

References.

(1) Poole K.M. Proc. Phys. Soc.B **66**, 542 (1953)
(2) Hall A.R., Dalton J.T. Hudson B, Marples J.A.C. in "Management of Radioactive Wastes from the Nuclear Fuel Cycle"(IAEA,Vienna ,1972) Vol.2, 3-14.

(3) Ewest E and Levi H.W. ibid. 15-25
(4) Mendel J.E. aross W.A. Robers F.P. Turcotte R.P. Katayama Y.B. and Westsik J.H. Jr. ibid 49-61
(5) Bursill L.A. Thomas J.M. and Rao K.J Nature **289**,157 (1981)
(6) Bursill L.A. Lodge E.A. and Thomas J.M. Nature **286**, 111 (1980)

E.H. Hirsch (1960) Image formation by electron bombardment of metal targets.
British Journal of Applied Physics, v. 11 (12), pp. 547-550, December 1960

E.H. Hirsch (1977) The growth of carbonaceous contamination on surfaces undergoing ion bombardment.
Journal of Physics D: Applied Physics, v. 10 (15), pp. 2069-2076, October 1977

E.H. Hirsch and T.R. Adams (1979) Ion bombardment of materials containing alkali metals or alkaline earths.
Journal of Physics D: Applied Physics, v. 12 (9), pp. 1621-1632, September 1979

E.H. Hirsch and T.R. Adams (1980) The Action of Water-Vapour on Ion Irradiated Alkali Silicate-Glasses.
Physics and Chemistry of Glasses, v. 21 (3), pp. 120-127, 1980

E.H. Hirsch (1980) A new irradiation effect and its implications for the disposal of high-level radioactive waste.
Science, v. 209 (4464), pp. 1520-1522, September 1980

E.H. Hirsch (1981) Stability of zeolites under electron irradiation.
Nature, v. 293 (5835), pp. 759, October 1981

Summary of Section E.

Thin Film Physics.

Paper no. 22. Two common methods for depositing thin films are vacuum evaporation and sputtering. Vacuum evaporation is a fast process, but the evaporant molecules arrive at the substrate only with thermal energy, and the film adherence to the substrate is frequently weak. By contrast the arrival energy of sputtered particles is typically in the range of a few keV, and the adherence is in general much better. But sputtering is a slower process than evaporation, and consequently there is a greater probability for the inclusion of impurities in the film during deposition.

In an effort to couple the rapidity of the evaporation process with high energy input into the deposited layer, this paper examines the deposition of Germanium films by high vacuum evaporation, combined with simultaneous bombardment by argon ions in the keV range, derived from a hot cathode plasma ion source. It is found that the ion bombardment has a dramatic effect on the film properties, greatly increasing the adherence and lowering the film stress. This occurs, although the ions constitute only about 4% of the total particle flux to the substrate.

The observations suggest that two factors combine in causing the greater adherence. Firstly an ion knock-on effect produces a thin layer of intermediate composition at the substrate surface, strengthening the interfacial bonding. Secondly the bombardment results in stress annealing of the deposit, but it is found that there must be a certain critical minimum ion current density for this stress reduction to occur. Details of this annealing effect will require further investigation.

Paper no. 23 investigates experimentally the annealing of stress in thin films by ion bombardment, reported in paper no.22. The results suggest an explanation of the annealing process in terms of the thermal spike, formed when an ion impacts on the substrate. In this spike the energy of the ion is dissipated by briefly raising the local temperature in a small region to a value high enough to cause permanent rearrangement of the atoms in the affected region [(1)].

The number of atoms participating in this rearrangement process during the lifetime of the spike, together with the dependence of this number on ion energy, can be calculated from a theory due to Seitz and Koehler [(2)]. On the other hand the experiments of paper no.23 establish that a critical minimum ion current density is required for film annealing to occur, and this critical ion density depends on ion energy through a simple power law. From this and the theory of Seitz and Koehler, one arrives at the intuitively satisfying conclusion that film annealing occurs when the ion current density is sufficiently high to ensure that all atoms deposited in the film undergo rearrangement in a thermal spike.

Paper no. 24 had its origin in the observation that freshly deposited films of magnesium fluoride exhibit large tensile stress following exposure to the atmosphere. Experiment showed that water vapour was the only atmospheric constituent responsible for the effect, and exposure to gases without dipole moment did not produce any stress.

Absolute measurements were made of the film stress as a function of water vapour pressure, and a model was developed, explaining the stress in terms of the interaction of molecular dipoles adsorbed on the walls of pores in the film. The model predicts that the stress induced by the adsorption of polar molecules is insignificant when the pore diameter is either very large or very small. But in an intermediate range from about 10^{-7} to 10^{-6} cm substantial stresses can be induced. From a practical point of view therefore this pore range should be avoided by suitable deposition techniques.

The adsorption stress is reversible. Therefore a porous film, mounted on a suitable elastic substrate such as a thin mica strip, constitutes the sensing element of a sensitive hygrometer. Experiment indicates a detection limit of about 5×10^{-4} Torr partial pressure of H_2O.

Paper no. 25 extends the work of paper no 24 from the adsorption stress caused by water molecules to that induced by a range of other polar organic adsorbates in magnesium fluoride films.

The observations again confirm the earlier conclusion that the stress is only produced by adsorption of molecules with a dipole moment. But the results also show that the simple model of paper no 24, which predicts the stress to be simply proportional to the square of the dipole moment, needs refinement. In particular, data for the three isomers of butyl alcohol, substances with not only the same molecular weight, but also having practically identical dipole moments, produce different adsorption stress. This indicates the importance of steric factors.

From observations of the time necessary for the stress to reach an equilibrium value it is concluded that the adsorbed molecules undergo a series of activated surface reactions.

References.

(1) Brinkman J.A. J.Appl. Phys. **25**, 961 (1954)
(2) Seitz F. and Koehler J.S. Solid State Phys. **3**, 305 (1956)

E.H. Hirsch and I.K. Varga (1978) The effect of ion irradiation on the adherence of germanium films.
Thin Solid Films, v. 52 (3), pp. 445–452, August 1978

E.H. Hirsch and I.K. Varga (1980) Thin film annealing by ion bombardment.
Thin Solid Films, v. 69 (1), pp. 99-105, June 1980

E.H. Hirsch (1977) Stress in porous thin films through absorption of polar molecules (and relevance to optical coatings).
Journal of Physics D: Applied Physics, v. 13 (11), pp. 2081-2094, November 1977

E.H. Hirsch (1982) On the origin of adsorption stress in thin porous films.
Journal of Physics D: Applied Physics, v. 15 (10), pp. 1991-1002, October 1982

Summary of Section F.

Vacuum Physics and associated Techniques.

Paper no. 26 describes a precision gauge for the measurement of either absolute pressure or pressure difference in the range up to 10 mm Hg .It was developed for the experiments on gas flow in porous media, described in paper no 27.

The gauge is essentially a mercury U-tube manometer, dimensioned so as to minimise meniscus effects. Mercury levels are determined by observing under optical magnification when fine points on two movable metal rods touch their mirror image in the liquid surface. The rods pass into the vacuum through Wilson sliding seals, and pressures are obtained by measuring differences in rod end position with a micrometer.

Paper no. 27. This paper describes an investigation into the flow of gases through porous media in the pressure regime intermediate between molecular and viscous flow. It was prompted by the need to develop a special purpose gas inlet for a mass spectrometer.

The work was undertaken because several investigators[1][2] had reported at times contradictory departures from the classical Adzumi equation[3], which predicts linear dependence of the gas flow on average pressure. Measurements were therefore made of the flow of various gases through porous pyrex disks having a range of average pore diameter. These confirmed a strong departure from linearity at low pressures. The results suggest an explanation in terms of sliding movement of gas layers adsorbed on the walls of the porous structure. Such movement constitutes a transport mechanism additional to that normally considered. Its effect is negligible in flow through conventional ducts, such as cylindrical pipes, but because of the high surface to volume ratio it becomes more important in porous media.

Paper no 28 describes a new vacuum gauge, the development of which originated from the earlier work on intermittent gas discharges (paper no.15). This gauge makes use of the fact that the electrode potential necessary to strike a glow discharge is higher than that needed to maintain it, and that the difference between these potentials is a function of the gas pressure. Consequently, if the glow discharge acts as the non-linear element of a relaxation oscillator, the electrode potential will vary periodically between striking and maintenance potential, and the gas pressure can be measured in terms of the relaxation frequency.

The construction of gauges operating on this principle can be made very simple and robust, rendering them particularly suitable for rocket-borne applications. They have in fact been used for upper atmosphere measurements.

Paper no. 29 is concerned with improving the performance of getter ion pumps for producing ultra-high vacuum. These pumps usually have a Penning cell configuration, in which the discharge current is linearly proportional to the pressure, and at ultra-high vacuum this current typically has a value of the order of 10^{-8} amps. Since the amount of gas removed is directly proportional to the current, this amount therefore becomes quite small at low pressure. The paper investigates the possibility of augmenting the gas quantity removed by injecting additional electrons from an auxiliary filament.

The results show that, because of the space charge conditions in the Penning configuration (paper no.4) the pumping speed does not rise linearly with the injected current ,but approximately with the cube root. Thermionic electron injection has the additional benefit of allowing pump operation at much lower magnetic field strengths and anode voltages than are needed for a cold cathode discharge.

Paper no 30 and no.31 arose from the need to obtain small, simple and ultra-high vacuum compatible sources of positive ions from non-gaseous materials. In paper no. 30 a simple electro-chemical process is used to produce thin layers of alkali tantalates on the surface of tantalum heater ribbons. When these ribbons are heated to low incandescence they act as very clean dispenser type sources of alkali ions. The performance of these ion sources is examined in detail.

Paper no 31 investigates the possibility of using surface ionisation for obtaining positive ions of metals with ionisation potential higher than that of the alkali metals. A source achieving this had been described by Zarabi and Satyam[4] who claimed to have obtained useful currents of Al^+, Sn^+ and Pb^+ by embedding these elements in a matrix of sodium silicate. Upon heating this matrix to low incandescence, it emitted a substantial positive ion current.

For elements such as Sn and Pb, with work functions exceeding 7 eV, to undergo surface ionisation, the work function of the emitter surface would have to be particularly high. In that case sodium, one of the matrix constituents, which has a much lower work function, would certainly also be surface ionised, and contribute to the ion output.

Unfortunately Zarabi and Satyam measured only the total ion current output, irrespective of species. Therefore to determine the suspected contribution of sodium, a sodium silicate matrix was charged with Al, and its ion output examined mass spectrometrically. The only species found were due to sodium and a potassium im-

purity. It therefore appears that the work function of the matrix is not sufficiently high to ionise Al, and that the output observed by Zarabi and Satyam was entirely due to the alkali content of the matrix.

Paper no 32 as well as papers no.33 and no.34 examine the performance of diffusion pump fluids. The work arose from incidental observations made in the course of other investigations. Paper no.32 investigates the origin of very regular fluctuations in the ultimate pressure of a diffusion pump operated with polyphenyl ether. It is found that the effect is due to the presence in the fore-vacuum of hydrogen. This is a product of thermal decomposition of the pump fluid, and when its partial pressure is sufficiently high, it produces an instability in the pump jet. As a result the mass flow through the jet is decreased. A substantial rise in pump heater input raises the level of mass flow sufficiently for the effect to be suppressed.

Paper no. 33 compares the performance of perfluoropolyether (Fomblin) and silicone diffusion pump fluids. Perfluoropolyether has the great advantage of not forming the otherwise ubiquitous contamination layers on particle irradiated surfaces, that were discussed in papers no.16 and 17.On the other hand, for reasons not clear, it generally achieves lower pumping speeds than conventional fluids. The primary aim of the experiments was to explain these lower speeds. In order to eliminate as far as possible incidental effects of pump geometry, measurements were made with two diffusion pumps of different design. Both pump types showed similar results in that the speeds obtained with Fomblin were lower..

The measurements indicate that two factors affect the performance. Firstly, because the molar specific heat of Fomblin exceeds that of other pump fluids, its mass flow rate through the pump at normal heater input is lower. Secondly, although the flow rate can be increased by raising the heater power, the advantage gained by this is counteracted by increased jet turbulence, which is more pronounced in Fomblin. Further investigation may show whether this turbulence can be reduced by improved pump jet design.

Paper no 34 deals with the observation, made earlier in my investigations, that when a diffusion pump using perfluoropolyether is operated into a ballast volume, the pressure rise in the ballast is faster then can be accounted for by the known outgassing and leak rates of the system being evacuated. In searching for a reason, it was discovered that a heavy decomposition product, clearly originating from the pump fluid, accumulates in the fore-vacuum. The most prominent mass spectrometrically determined components of this product include CO_2, CF_3 and C, but these are considered to be fragments of a molecule whose mass exceeds the range of 100 mass units of the spectrometer. The breakdown product can be partially readsorbed in the bulk of the pump fluid, where it is held in a weakly bound state. After prolonged operation its presence leads to a gradual change in the pump fluid.

Detailed observations of the processes of breakdown and re-absorption were made, and a rate equation for the process was developed.

References.

(1) Carman P.C. and Lund L.M. Proceedings of the Second International Conference on Peaceful Uses of Atomic Energy, Geneva, **4**, 359 (1958)
(2) Grove D.M. and Ford M.G. Nature **182**, 999 (1958)
(3) Adzumi H. Bull Chem. Soc. Japan **12**, 304 (1937)

E.H. Hirsch (1959) Precision pressure gauge for the range 0 to 30 mm of mercury.
Journal of Scientific Instruments, v. 36 (11), pp. 477, November 1959

Flow of Gas through Porous Media in the Region between Molecular and Viscous Condition

E. H. HIRSCH
Weapons Research Establishment, Salisbury, South Australia
(Received August 18, 1960; and in final form, January 16, 1961)

Experiments on the flow of gases through porous Pyrex disks at pressures in the range of a few mm Hg are described. For air, hydrogen, and carbon dioxide the specific flow is found to be given by

$$Q=\frac{A}{(MT)^{\frac{1}{2}}}+\frac{B}{\eta T}\bar{p}+\frac{C}{M^{\frac{1}{2}}}\{1-\exp[\alpha_0-\beta T^{\frac{1}{2}}]\bar{p}\}$$

The significance of this result is discussed.

I. INTRODUCTION

IN discussing the flow of gas through a tube, it is usual to distinguish two different basic processes, namely intermolecular collisions and collisions between gas molecules and the walls of the containing vessel. It is then possible to divide the flow into several regimes which differ in the relative importance of these two types of collisions.

At sufficiently low pressure, where the mean free path λ is large compared with the tube diameter d, i.e., for large values of the Knudsen number $K=\lambda/d$, intermolecular encounters are rare and the gas transport is governed by wall collisions.

Under these conditions of so-called molecular flow, it can be shown[1] that the specific flow, i.e., the amount of gas in moles transported per sec per unit pressure difference, is given by

$$Q=\frac{d^3}{3L}\left(\frac{\pi}{2MRT}\right)^{\frac{1}{2}}\left(\frac{2}{f}-1\right) \quad \text{(molecular flow)}, \quad (1)$$

where d=tube diameter cm; L=tube length cm; M=molecular weight of gas; R=gas constant; T=temperature °K; f=fraction of diffusely reflected molecules. Equation (1) represents the flow well under conditions characterized by a value of K of about 10 or more. At the other end of the pressure range ($K<0.01$), however, intermolecular collisions will predominate and the flow is very accurately described by the well-known Poisseuille equation

$$Q=(\pi d^4/128L\eta RT)\bar{p} \quad \text{(viscous flow)}, \quad (2)$$

where η=viscosity (poise); $\bar{p}$=mean pressure=$[(p_1+p_2)/2]$ (dynes); p_1, p_2=pressures at the ends of the tube. In the pressure region where the mean free path λ, though small, is not altogether negligible, ($0.01<K<0.1$) it becomes necessary to introduce a "slip-flow" correction[2] into Eq. (2), which then assumes the form

$$Q=\frac{\pi d^4}{128L\eta RT}\bar{p}+\left(\frac{\pi d^3}{16L}\right)\left(\frac{\pi}{2MRT}\right)^{\frac{1}{2}} \quad \text{(slip flow)}. \quad (3)$$

It will be noted that although the slip-correction term in Eq. (3) is of the same form as the molecular-flow term [Eq. (1)], it differs from the latter by the numerical factor $3\pi/16$. It is because of this factor that Eq. (3) does not reduce to Eq. (1) as $\bar{p}\rightarrow 0$, a discrepancy which arises from the fact that the slip theory, because of its inherent approximations, must fail when λ becomes comparable with d. In fact, up to the present no satisfactory theoretical treatment of gas flow is available for the "transition region," which we may roughly place at $0.1<K<10$.

While we have so far only discussed gas transport through cylindrical tubes, the above considerations can, at least in principle, be extended to cover the case of porous media, which are considered essentially as bundles of short capillary tubes connected in series-parallel.

Using this model, the specific flow through a porous body is then, in analogy with Eq. (3), given by an expression of the general form[3,4]

$$Q=a+b\bar{p}, \quad (4)$$

where a and b are coefficients which, apart from the properties of the gas, also take into account the geometry of the porous structure.

The linear relationship between specific flow and mean pressure, which is predicted by Eq. (4), in fact has been confirmed by a number of observers, at least in the region of reasonably high pressures.[4]

In the low-pressure domain, on the other hand ($\bar{p}$ usually of the order of a few mm Hg), discrepancies which point to insufficiencies in the classical flow equations have been noted.

Thus Berman and Lund,[5] while observing low-pressure linearity of the specific flow curve, report gas and temperature dependence of the Knudsen permeability, which should be dependent on geometry only.

Studying the flow of H_2, air, CO_2, and CF_2Cl_2

[1] M. Knudsen, Ann. Physik **28**, 75, 999 (1909).
[2] E. H. Kennard, *Kinetic Theory of Gases* (McGraw-Hill Book Company, Inc., New York, 1938), p. 293.
[3] H. Adzumi, Bull. Chem. Soc. Japan **12**, 304 (1937).
[4] P. C. Carman, Proc. Roy. Soc. (London) **A203**, 55 (1950).
[5] A. S. Berman and L. M. Lund, *Proceedings of the Second International Conference on Peaceful Uses of Atomic Energy, Geneva* (United Nations, 1958), Vol. 4, p. 359.

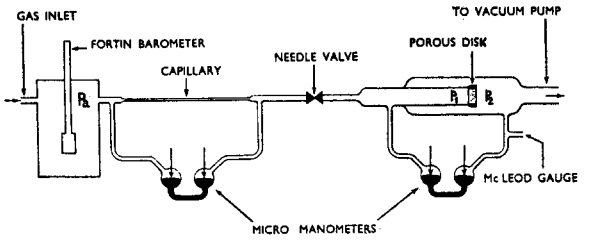

FIG. 1. Diagram of flow apparatus.

through a bed of chromite powder, Carman[4] finds evidence of an increase of gradient of the specific flow curve towards smaller $\bar{p}$. A similar tendency is noted to a more pronounced extent by Barrer and Grove[6] for the flow of NH_3, CCl_4, and SO_2 through an analcite column, but for the noble gases they observe a flattening of the curve. In contrast to this, Grove and Ford,[7] again using the noble gases, but with ceramics and graphites as porous media, report the existence of minima, the position of which is gas dependent. This diversity of findings makes it desirable to gain further knowledge regarding the nature of the departures from the classical laws.

It is the purpose of the present work to study the dependence of nonlinearities in the specific flow curve on pore diameter and temperature for the flow of air, hydrogen, and carbon dioxide through porous Pyrex disks.

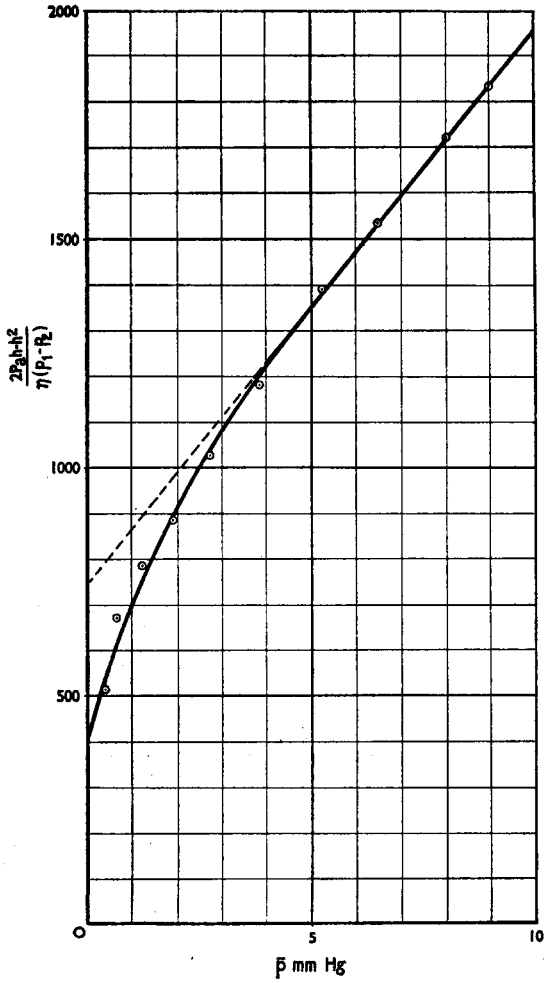

FIG. 2. Specific flow for air at room temperature.

II. EXPERIMENTAL ARRANGEMENT

Figure 1 shows the experimental arrangement schematically. The test gas was dried in a large chamber at about atmospheric pressure P_a and accurately measured on a builtin Fortin barometer. From the drying chamber the gas passed through a flow meter consisting of a glass capillary (0.67 mm mean diam and 705 mm in length). The pressure h across the capillary could be measured with a micromanometer[8] which had been specially developed to extend the experimental range to sufficiently low mean pressures.

A needle valve permitted control of the flow through the porous body, and a second micromanometer served to measure the pressure difference p_1-p_2 across the latter. Furthermore, a McLeod gauge was arranged for the determination of p_2, the pressure on the pump side of the porous structure.

Since the mean pressure in the flow meter capillary was practically atmospheric the flow through it was, in view of its dimensions, purely viscous, i.e., the amount flowing per sec was proportional to $(2P_ah-h^2)/\eta$, so that for a particular gas the quantity $(2P_ah-h^2)/[(p_1-p_2)\eta]$ was a measure of the specific flow through the porous medium.

Experiments were carried out in commercial Pyrex filter disks cemented by means of Apiezon wax into glass mountings, as shown.

III. EXPERIMENTAL RESULTS

The first set of experiments was carried out with air at room temperature using Pyrex filter disks of various pore diameters.

In all cases the general character of the specific flow curve was as shown in the example of Fig. 2, which represents results for a disk of porosity grade 1 (100–120 μ mean pore diameter).

With increasing mean pressure the gradient steadily decreased until at a pressure of a few mm Hg it approached a constant value which, as will be shown below, corresponded to the slope due to viscous flow.

It was found that the experimental curves were well represented by equations of the form

$$Q=a+b\bar{p}+c[1-\exp(-\alpha\bar{p})], \qquad (5)$$

where a, b, c, and α are constants. The nonlinear term in Eq. (5) constitutes a flow component which is

[6] R. M. Barrer and D. M. Grove, Trans. Faraday Soc. **47**, 826 (1951).
[7] D. M. Grove and M. G. Ford, Nature **182**, 999 (1958).
[8] E. H. Hirsch, J. Sci. Instr. **36**, 477 (1959).

additional to the molecular and viscous terms, and the contribution of which rises from zero at $\bar{p}=0$ to an asymptotic value c, closely approached at a pressure of several mm Hg.

Table I summarizes the experimental results obtained with porous disks of various grades. The pore sizes given are as stated by the manufacturers, and the constants a, b, and c have been normalized to correspond to a porous body of 1 cm² in cross section and 1 cm in length.

As is to be expected, the values of a and b both decrease with pore diameter d, and the same applies to the coefficient c of the nonlinear term.

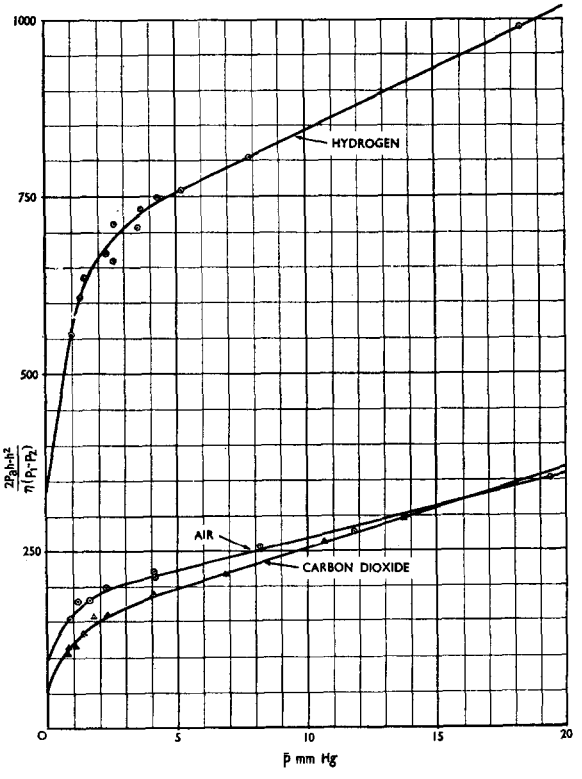

FIG. 3. Specific flow for H_2, CO_2, and air.

On the other hand, there is no systematic variation of the exponent α with pore diameter, and the changes of α shown in Table I, which are outside experimental error, probably result from differences in pore shapes for various grades of filter disks.

It is noteworthy that although experiments ranging over two orders of magnitude of d were made, α remained constant within a factor of 3. The pressure variation of the nonlinear term in Eq. (5) is thus roughly the same for different pore diameters, i.e., the flow mechanism represented by this term is one which is not a function of the Knudsen number but rather of the mean pressure.

It is natural to identify the first two terms of Eq. (5) with the contributions due to molecular and viscous flow, in which case the coefficients a and b should vary

TABLE I. Flow constants for various pore diameters (air at room temperature).

Porosity grade	Average pore diameter, μ	a	b	c	α	$\frac{c}{c+a}$
1	100–120	414	118.0	364.0	0.75	0.47
2	40–50	114	18.7	137.0	1.25	0.55
3	20–30	66	8.55	114.0	1.50	0.63
4	5–10	44	1.26	26.6	0.50	0.38
5	not larger than 1.5	7.0	0.0266	3.06	0.60	0.30

with temperature, molecular weight, and viscosity according to Eqs. (1) and (2), respectively.

In order to check this point and also to gain more information regarding the nature of the nonlinear term, additional experiments were made using H_2 and CO_2; a series of measurements with air over the temperature range from 293°–773°K were also made. Figure 3 shows the specific flow of H_2, CO_2, as well as air, through a disk of porosity 3 ($d=20-30\,\mu$), and the nonlinearity is seen to occur in all three cases. The numerical values of the flow constants obtained from these measurements are given in Table II.

The constancy of the products $aM^{\frac{1}{2}}$ and $b\eta$ is, of course, in accordance with Eqs. (1) and (2). In addition, Table II also shows that $cM^{\frac{1}{2}}$ is a constant, i.e., the coefficient c of the nonlinear term varies as the molecular flow term a for different gases.

The exponential factor α also varies somewhat with the nature of the gas, but its variation does not appear to be a simple function of elementary properties such as molecular weight and viscosity.

Lastly, the temperature dependence of the flow of air was studied on a filter disk originally of porosity 3,[9] fused into a Pyrex envelope. The results of these measurements are given in Fig. 4 and Table III.

The products $aT^{\frac{1}{2}}$ and $b\eta T$ are both constant, and in addition the coefficient c is found to be independent of temperature. There is, however, a systematic change of α with T, which becomes smaller with increasing temperature. Figure 5 shows that within experimental error $\alpha=\alpha_0-\beta T^{\frac{1}{2}}$.[10]

TABLE II. Flow constants for air, H_2, CO_2 (room temperature, filter disk porosity 3).

	M	a	b	c	α	$\eta(\times10^4)$	$a(M)^{\frac{1}{2}}$	$b\eta(\times10^8)$	$c(M)^{\frac{1}{2}}$
Air	29	66	8.55	114	1.5	1.81	356	15.5	614
H_2	2	251	17.2	425	1.15	0.88	354	15.1	599
CO_2	44	54	10.7	91	0.95	1.46	358	15.6	603

[9] During the glass blowing and subsequent annealing a certain amount of fusing of the porous disk was unavoidable. Its porosity was therefore eventually not that of standard porosity 3, and results for this disk (35 mm diam and 3 mm thickness) are not normalized to unit cube.

[10] The author is indebted to Dr. W. Schwietzke for drawing his attention to this fact.

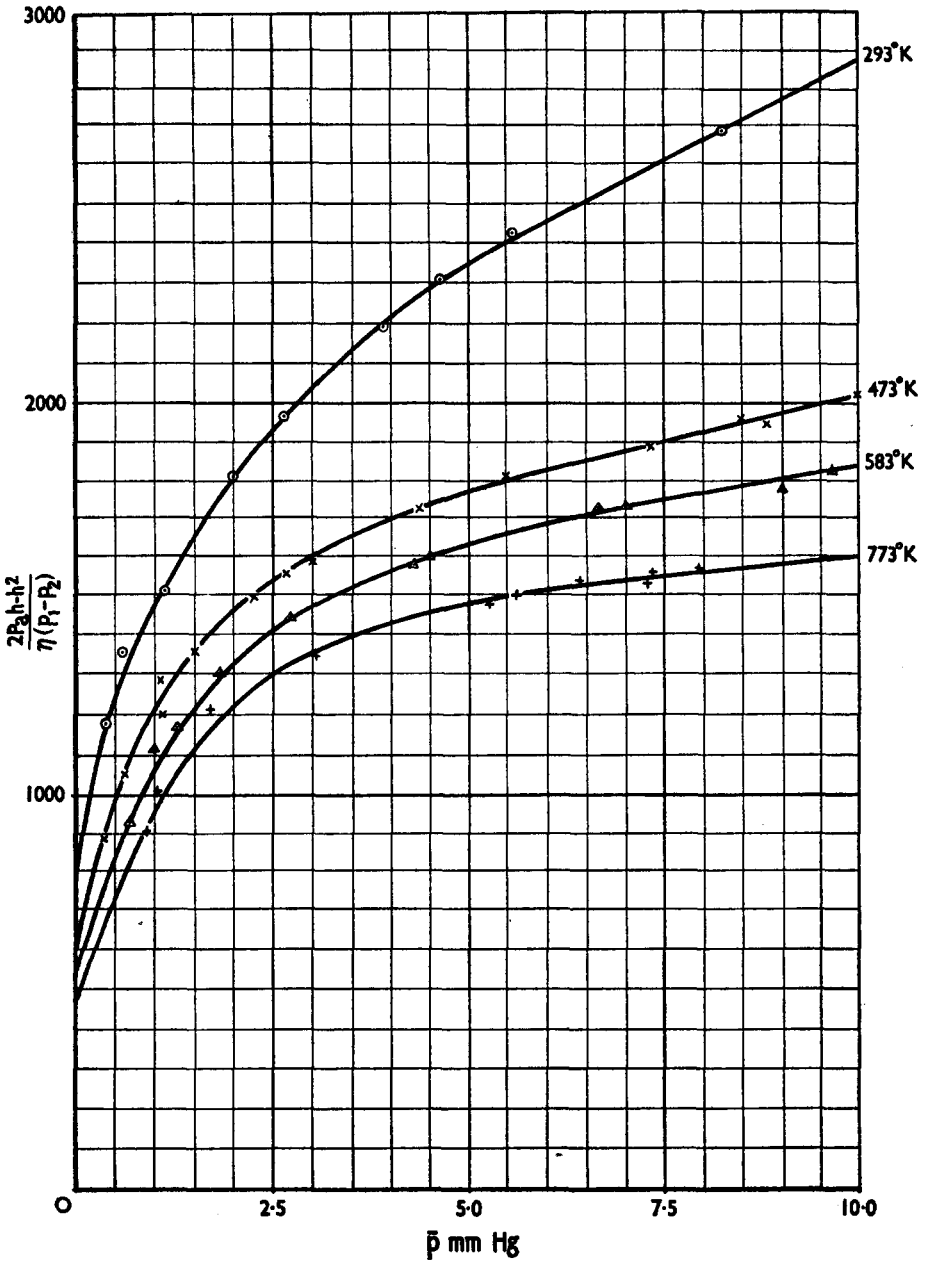

FIG. 4. Variation of specific flow with temperature (air).

The preceding results may be summarized by writing Eq. (5) in the form

$$Q=\frac{A}{(MT)^{\frac{1}{2}}}+\frac{B}{\eta T}\bar{p}+\frac{C}{M^{\frac{1}{2}}}\{1-\exp[-(\alpha_0-\beta T^{\frac{1}{2}})\bar{p}]\}, \quad (6)$$

TABLE III. Flow constants for air at various temperatures.

T°K	a	b	c	α	$aT^{\frac{1}{2}}(\times10^{-2})$	$b\eta T(\times10^{-2})$
296	780	118	920	1.0	134	632
473	610	51.0	910	0.9	132	620
583	555	36.7	925	0.7	134	640
773	485	22.8	910	0.7	135	631

where A, B, and C are constants for a given porous medium, decreasing with decreasing pore diameter, but being independent of the nature of the gas.

The exponential coefficient $\alpha=(\alpha_0-\beta T^{\frac{1}{2}})$, on the other hand, varies for different gases, and any change of α with the properties of the porous medium appears unrelated to the pore diameter and is presumably caused by variations in pore shape.

The first two terms of Eq. (6) are clearly the contribution of molecular and viscous flow, but the third term represents a flow component which is characteristic of porous media and is not normally observed in the flow through cylindrical tubes.

In order to verify this latter point, flow measurements

were made on a disk of about 2.5 mm thickness, carrying 60 straight holes of approximately 0.1 mm diam. Except for the fact that the disk constituted a number of "long" cylindrical tubes in parallel, this experiment was in other respects, such as hole diameter and pressure range used, quite comparable to measurements on a filter disk of porosity 1. While in the latter case the presence of the third, nonlinear term had been definitely established, the relation between Q and $\bar{p}$ for the straight holes was linear within experimental accuracy (see Fig. 6).

IV. DISCUSSION OF RESULTS

The presence of a nonlinear term in the specific flow equation is not only of interest in connection with the problem of the transition of molecular to viscous flow, but it can also assume importance when gas permeability data are used for the derivation of quantities such as particle size in the "subsieve range" or the determination of specific area.[11]

These problems involve finding the viscous and molecular flow components from the slope and ordinate intercept of the specific flow curve.

Now the form of the nonlinear term is such that beyond a certain pressure, depending on the value of α, and in our particular case ranging from about 3.5–9.5 mm Hg, this term becomes sensibly constant.

If experimental points are taken at higher pressures only, then the nonlinearity is masked and extrapolation to $\bar{p}=0$ will yield an ordinate intercept

$$a_1=[A/(MT)^{\frac{1}{2}}]+(C/M^{\frac{1}{2}}),$$

which exceeds the molecular term by $C/M^{\frac{1}{2}}$. Depending on the magnitude of C, the error may be quite considerable, and in some of our experiments could exceed 100%.

It is interesting to consider in this context the results of Carman,[4] who finds that for high values of d/λ the specific flow curve is always linear, and that occasionally there is a departure from linearity near $d/\lambda\sim 1$ but that no marked change of gradient is ever experienced.

Analysis of his data shows, however, that while he obtained perfect linearity in one instance from $d/\lambda=0.038$ up to $d/\lambda=1.4$ and in another from $d/\lambda=0.3$ to $d/\lambda=11$, no significant readings were taken below approximately 30 mm Hg.

In those cases where signs of nonlinearity were in fact found, these occurred only at somewhat lower values of mean pressure, although the range of d/λ was roughly as above.

These facts are of course in agreement with our finding that the nonlinearity is not in any way related to the Knudsen number, being instead dependent on the mean pressure, and only observable below a certain $\bar{p}$.

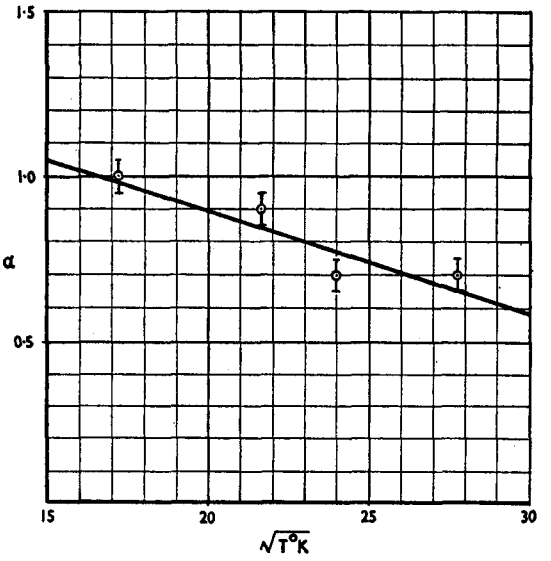

FIG. 5. Variation of α with temperature.

Lastly, we may consider a possible transport mechanism which may account for the nonlinearity to be observed in the flow of gas through a porous medium, but which is insignificant if a cylindrical capillary is involved.

Since our experiments have shown that the mechanism can be operative under conditions where intermolecular collisions are very rare events, it is reasonable to associate it with collisions between molecules and the containing walls.

The only point at which the effect of gas-wall interaction enters the gas flow Eqs. (1) and (2) is through the quantity f, introduced by Maxwell[12] to take into account the degree of diffuse reflection of molecules due to random irregularities in the microgeometry of the containing wall.

There is, however, strong evidence to show that the nature of f is more complex than that of a factor merely representing geometry.

While numerical values of f available are rather

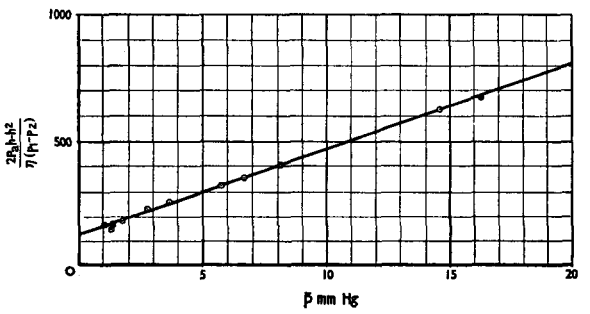

FIG. 6. Specific flow through system of cylindrical capillaries (air).

[11] P. C. Carman, *Flow of Gases through Porous Media* (Butterworths Scientific Publications Ltd., London, 1956), p. 84.

[12] J. C. Maxwell, *Collected Scientific Writings* (Cambridge University Press, Cambridge, England, 1873), Vol. 2, p. 704.

few[13,14] they indicate clearly a dependence of f both on the nature of the wall and the interacting gas.

The fact that the slip term [Eq. (3)] does not numerically converge to the Knudsen term as $\bar{p} \rightarrow 0$, also points strongly to a pressure dependence of the wall interaction represented by the factor $[(2/f)-1]$.

Furthermore, Barrer and Grove[6] report a small but significant decrease of the Knudsen permeability with temperature. This is in qualitative agreement with the observed temperature variation of

$$[C/M^{\frac{1}{2}}]\{1-\exp[-(\alpha_0-\beta T^{\frac{1}{2}})\bar{p}]\}$$

in the present work. Berman and Lund[5] observe a change of the Knudsen term in the same direction for helium, but an opposite tendency for the other noble gases.

In order to account for these various effects it would seem necessary to introduce a more elaborate model for the wall interaction than that used by Maxwell, who considered the walls to be perfectly rigid. In actual fact it is well known, however, that even under conditions of high vacuum, a solid surface is rapidly covered by a layer of adsorbed gas molecules which are capable of migrating along the surface.[15] Thus, rather than colliding with a solid wall of "infinite" mass, the molecule in undergoing a wall collision can interact with an adsorbed molecule or molecular complex having a mass comparable to its own.

A transfer of tangential momentum to the adsorbed layer will thus take place; on the average, this will have a resultant in the direction of gas flow. A certain amount of gas transport can therefore occur through the ensuing sliding motion of the adsorption layer. It is, in fact, not unreasonable to assume that it is through this motion of the adsorbed layer that random diffusive flow at low pressures is eventually transformed into ordered laminar streaming.

A rough calculation shows that in a typical porous body, and in the pressure region of interest here, the amount of gas adsorbed on the walls is of the same order of magnitude as that present in the gas phase, within the volume bounded by the adsorbing walls.

In order to estimate the number of molecules adsorbed, we may adopt the typical value of 10^4 for the specific area of the porous medium, i.e., for the wall area in cm^2/cm^3 enclosed volume. If, furthermore, the conservative value 10^{14} is taken as the number of adsorption sites per cm^2, a coverage of only 1% of a monolayer will correspond to 10^{16} adsorbed molecules. This is of the same order as the number of air molecules per cm^3 at room temperature and 1 mm Hg pressure, which is approximately 3.5×10^{16}.

Under these conditions, therefore, movement of the adsorption layer may reasonably be expected to yield a significant contribution to the total flow.

One might expect the contribution of film transport of the type proposed here to be more pronounced the larger the specific area, in which case the ratio $c/c+a$ should increase with decreasing pore diameter (assuming a substantially constant void fraction).

Table I shows that this is not the case and that there is in fact no definite trend of $c/c+a$ with pore diameter d.

It must be remembered, however, that any change in d automatically implies changes in other relevant factors such as pore shape, length of path over which film transport takes place, and change in the effects of local pressure variation due to nonuniformity of pore cross section.[16]

The net effect of all these variations is of course difficult to assess, but it need not necessarily result in larger film transport for larger specific area.

In the case of flow through straight capillaries one would, however, expect film transport to make only a negligible contribution.

Not only is the specific area small (about 40 for a tube of 1 mm in diameter), but in addition a molecule, in passing through the capillary, will make, on the average, a considerably smaller number of wall collisions than in a porous medium.

Molecules on trajectories more or less parallel to the capillary axis in fact have a finite probability of passing through without a single collision, i.e., without contributing to film transport in any way, a case which does not arise in a porous medium.

Generally the temperature and pressure dependence of film transport can be expected to vary under different experimental conditions. We are dealing here with a complex phase-boundary phenomenon into which enter a number of elementary processes such as adsorption and evaporation of gas molecules, surface migration, and, in some instances, dissociation of adsorbed molecules and the formation of molecular complexes.

All these processes have their individual activation energies and rate constants, and the over-all variation of film transport with $\bar{p}$ and T will depend on the relative magnitude of these various individual constants, i.e., it may differ for various adsorbent-adsorbate systems.

A similar state of affairs is found in other phase-boundary phenomena,[17] and while Eq. (6) adequately describes flow under the conditions of the present work, a general flow equation would require more detailed knowledge of the various surface effects involved, than is available at the present time.

ACKNOWLEDGMENTS

The author wishes to thank Dr. W. Schwietzke for his interest and encouragement throughout the work. Publication is made with the permission of the Chief Scientist, Australian Defence Scientific Service, Department of Supply, Melbourne, Australia.

[13] H. Adzumi, Bull. Chem. Soc. Japan **14**, 343 (1939).
[14] R. Millikan, Phys. Rev. **21**, 217 (1923).
[15] J. A. Becker, Advances in Catalysis **7**, 136 (1953).
[16] T. H. Chilton and A. T. Colburn, Ind. Eng. Chem. **23**, 913 (1931).
[17] R. Ash and R. M. Barrer, Phil. Mag. **4**, 1197 (1959).

Vacuum Measurements by Means of Alternating Gas Discharges

E. H. HIRSCH
Weapons Research Establishment, Salisbury, South Australia
(Received August 10, 1959; and in final form, October 2, 1961)

A pressure gauge for the range from several mm Hg down to the micron region is described. The new gauge, based on the properties of alternating gas discharges, measures pressure in terms of the frequency of a relaxation oscillator incorporating as the nonlinear element a glow discharge between electrodes immersed in the gas, the pressure of which is to be determined. A stability of 1% has been obtained; the robustness and simplicity of the instrument render it particularly suitable for rocket-borne measurements at high altitude.

INTRODUCTION

THIS paper describes a new type of pressure gauge for use from several mm Hg down to high vacuum.

The instrument is free from the zero drift associated with Pirani gauges, and does not entail the measurement of very small direct currents as in the Alphatron. In view of the simplicity of construction of the gauge element itself and of its associated electrical circuit, the gauge offers advantages for measurement of atmospheric pressure at high altitude.

THEORY OF OPERATION

The gauge is based on the fact that in a given gas the voltage V_F at which a glow discharge is fired between two electrodes of a given geometry is a function of the gas pressure p and that, once the discharge has set in, the applied voltage may be decreased until the discharge is finally extinguished at a voltage V_E, which is again a function of pressure.

If the electrodes are connected across a condenser which is charged through a high resistance R from a voltage source (see Fig. 1), the system will in general undergo relaxation oscillations, the condenser being alternately charged through R to a potential V_F and discharged through the electrode gap, until the voltage across the electrodes has dropped to the value V_E. Through its dependence on V_F and V_E, the frequency of oscillations f is a function of pressure and may be used to measure the latter. This is conveniently done by inserting a resistor r as shown and counting the voltage pulses which are developed across it every time the discharge is fired. Alternatively, the pulses can be integrated and the pressure reading presented in the form of a dc voltage.

To arrive at an expression for f, the glow discharge in the circuit of Fig. 1 may be represented by a time-varying resistance R_i. Neglecting the effect of the small resistance r, the condenser potential V_c is given by

$$\frac{dV_c}{dt}=\frac{1}{(C+C')}\left\{\frac{V}{R}-V_c\left[\frac{1}{R}+\frac{1}{R_i}\right]\right\}. \tag{1}$$

Here V is the applied voltage and C' represents the self-capacity of the discharge due to the presence of charged particles in the interelectrode gap.[1,2]

Because of the complicated variation of R_i with time, an exact integration of Eq. (1) is not possible. A solution can, however, be obtained under the simplifying assumption that, for the duration of the glow discharge, R_i assumes a constant value which is small compared with that of the charging resistor, while for the rest of the cycle R_i is taken to be infinite.

Under these conditions, the repetition frequency is readily found as

$$f=\left\{(C+C')\left[R\ln\left(\frac{1}{1+\delta/(V-V_F)}\right)+R_i\ln\left(\frac{V_F}{V_F-\delta}\right)\right]\right\}^{-1}, \tag{2}$$

where $\delta=V_F-V_E$ represents the difference between the critical potentials. Thus f is a function of δ and therefore in turn also a function of p.

In order to see the type of calibration curve, i.e. frequency-pressure relation, to be expected from the arrangement, consider Fig. 2 which shows typical curves of V_F, V_E, and δ against pressure.

The quantity δ is seen to decrease steadily with decreasing pressure, so that, as p decreases, the logarithmic terms in Eq. (2) both tend to $\ln 1=0$ and we should expect the frequency to rise monotonically with decreasing pressure. In actual fact, this prediction is only fulfilled at

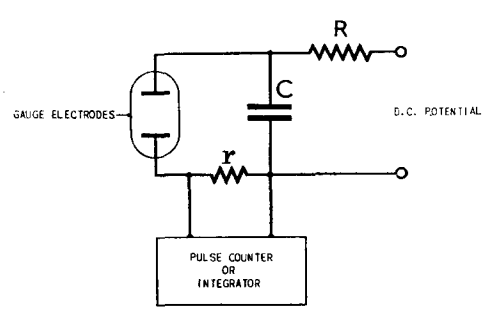

FIG. 1. Basic gauge arrangement.

[1] G. Francis, *Encyclopedia of Physics*, edited by S. Flügge (Springer-Verlag, Berlin, Germany, 1956), Vol. 22, p 188.
[2] H. Ritow, J. Electronics and Control 4, 111 (1958).

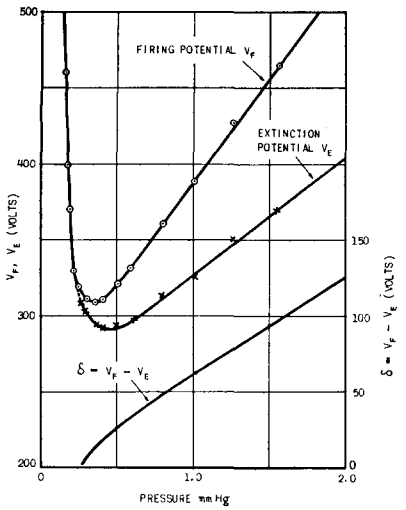

FIG. 2. Typical variation of V_F, V_E, and δ with pressure.

reasonably high values of pressure, since a typical experimental curve is as shown in Fig. 6.

Here, after an initial rise in frequency as predicted by Eq. (2), the curve reaches a maximum after which the frequency drops quite sharply. The cause of this behavior lies in two factors which were disregarded in the simple theory leading to Eq. (1), but which assume importance in the range of lower pressures.

Firstly, the internal resistance of the discharge R_i is not constant throughout. As the discharge becomes weaker at lower pressure, the value of R_i becomes progressively larger, which will tend to reduce the frequency.

A second factor operating in the same direction is the pressure dependent variation of the self-capacity C'. At high pressures this capacity is normally quite small. Experiments to be reported more fully elsewhere have shown however that, with decreasing pressure, C' rapidly increases and eventually becomes larger than the capacity of the external condenser C, thus bringing about a sharp decrease in the pulse repetition rate.

Having discussed the general character of the calibration curve, it now remains to consider the factors governing the working range of the gauge.

For any particular gauge geometry the highest pressure that can be measured depends on the available dc voltage, since this must naturally be larger than the firing potential required for the pressure in question (see Fig. 2).

Because of the shape of the firing potential curve, a similar limitation exists also, in principle, at the low pressure end of the range, but in practice, before this limitation can become operative, a second factor, namely the increase of R_i with decreasing pressure, comes into play.

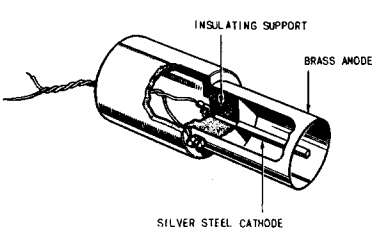

FIG. 3. Cylindrical gauge structure.

As a result of this increase in internal resistance, a situation is ultimately reached where the rate of discharge of the condenser through the gas is counterbalanced by the rate at which charge is supplied to it from the dc source. This occurs when

$$(V-V_c)/R=V_c/R_i, \tag{3}$$

which by Eq. (1) is also the condition for $dV_c/dt=0$, i.e., for the relaxation oscillations to cease. A continuous discharge then develops and the low pressure limit of the arrangement as an alternating discharge gauge has been reached.

Since both the firing potential and the internal resistance R_i depend on the geometry of the gauge electrode system, it follows that the operating range can be modified by suitable changes in the gauge geometry; in the following, experimental results are presented showing the performance of gauges using several different types of electrode system.

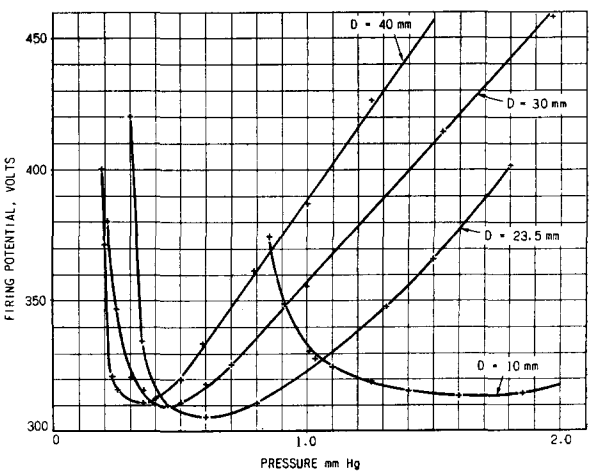

FIG. 4. Firing potential of cylindrical gauge as function of pressure for various values of anode diameter.

EXPERIMENTAL RESULTS

A. Cylindrical Gauges

Initial experiments were made with gauges of a concentric cylindrical geometry of particularly simple and robust construction as shown in Fig. 3.

The gauges consisted essentially of a brass tube, 45 mm in length, which served as anode, and a cathode, consisting of a 3-mm-diam silver steel rod, arranged along the axis of the anode cylinder. The whole was mounted on a simple insulating support.

As a rule this type of gauge was operated with a 5000-$\mu\mu$f condenser and a 20-meg charging resistor. The voltage pulses were derived across a 30 000-ohm resistor and were

typically about 50 μsec wide with an amplitude ranging from about 2 v to over 100 v, depending on pressure.

The repetition frequency, which typically lay in the lower audio range, was measured by feeding the pulses into an electronic counter timed over a fixed interval.

Normally, experiments were made at room temperature using dry air. The pressure was measured on a standard McLeod gauge which allowed reproducibility of readings within 1% over the relevant range, and which was connected to the system through a liquid air trap.

It was found that, at constant pressure, the pulse repetition rate of the alternating discharge gauge was stable within 1% and the calibration curve showed very good reproducibility over several months, during which time no disturbing effects due to sputtering were observed.

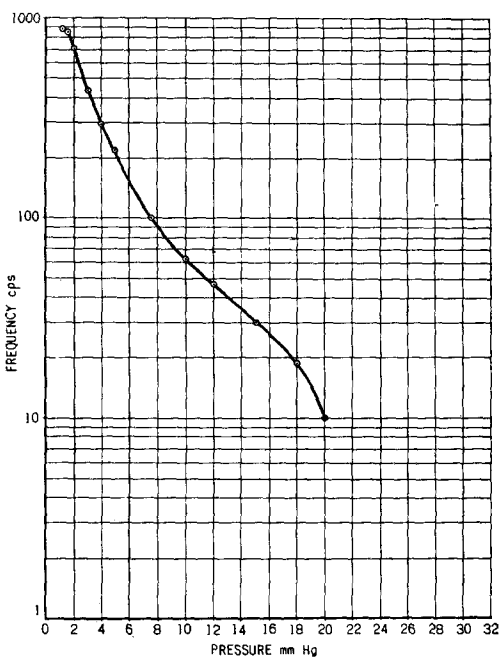

FIG. 5. Calibration curve for cylindrical gauge, 10-mm anode diameter, operating voltage 780 v.

To investigate the effect of ambient temperature, one gauge was mounted in an envelope filled to a pressure of 1 mm Hg at room temperature. The envelope was then cooled by solid carbon dioxide and by means of liquid air; in each case the repetition frequency was found to be independent of ambient temperature. In common with other vacuum gauges such as ionization, Pirani or viscosity gauges, which are not of the membrane or liquid manometer type, the instrument is therefore, strictly speaking, not a pressure but a density gauge. This distinction is of little consequence in the usual applications at room temperature, but must be borne in mind when measurements are to be made under conditions of varying temperature such as in rocket-borne upper atmosphere measurements.

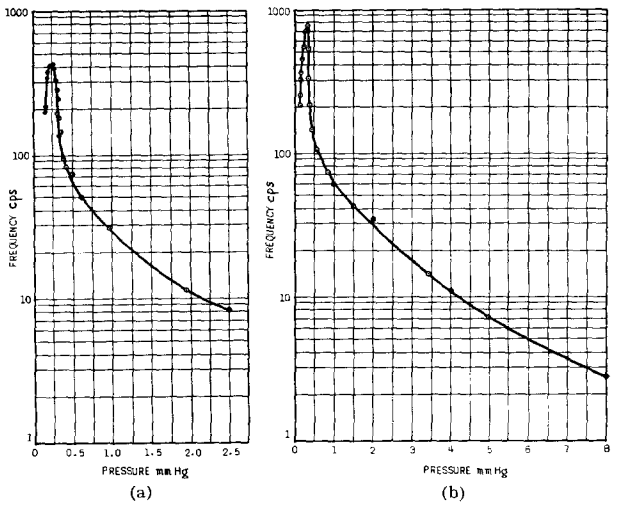

FIG. 6. Calibration curve for cylindrical gauge, 40-mm anode diameter, operating voltage (a) 600 v, (b) 900 v.

Turning now to a more detailed discussion of the characteristics of cylindrical gauges, Fig. 4 shows firing potential curves for various values of anode diameter D.

It is seen that the smaller the value of D, the lower will be the firing potential on the high pressure side of the curve minimum, while on the low pressure side the reverse is the case. Consequently, for a given applied voltage the operating range of the gauge can be extended to higher pressure by adopting a small anode diameter. As an example, Fig. 5 shows the calibration curve of a 10-mm-diam gauge which, using 780 v, extends from 20 mm Hg down to 1 mm Hg. At this lower pressure, the discharge current becomes so small that the condition of Eq. (3) holds and a continuous discharge results before the maximum in the curve is reached.

Experiments show that, by increasing the anode diameter, a stronger low pressure discharge and therefore a corresponding extension of the range can be obtained. At constant applied voltage this is, of course, attended by a range contraction on the high pressure side. As an example,

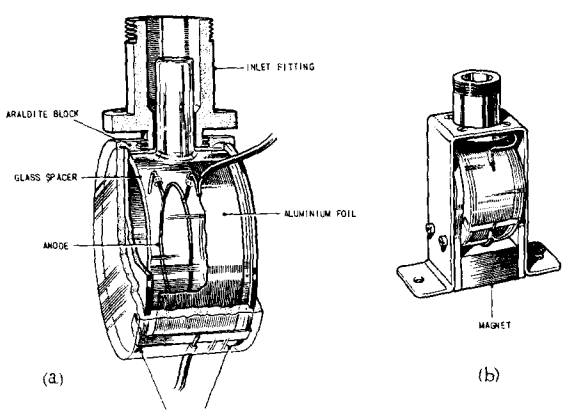

FIG. 7. Construction of gauge for low pressure operation using Penning type electrodes.

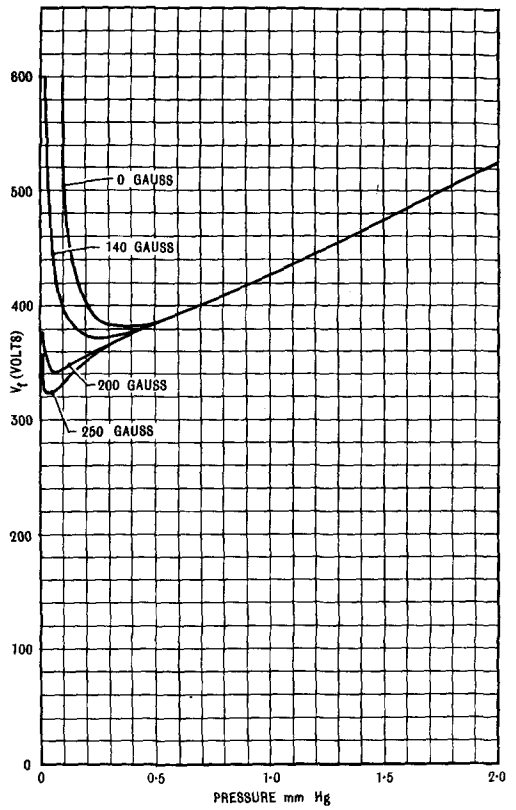

FIG. 8. Firing potential of low pressure gauge as function of pressure for various values of magnetic field strength.

Fig. 6 shows calibration curves for a 40-mm-diam gauge for 600 and 900 v, respectively. In both cases, the low pressure limit is about 0.15 mm Hg, while the upper end of the range is approximately 2.5 mm Hg for 600 v and 8 mm Hg for 900 v.

B. Gauges Using Penning Type Structures

Cylindrical gauges of the type described above provide a simple and reliable means of measuring pressure in the millimeter and submillimeter region, but extension of their working range to the micron region has proved difficult. The discharge intensification required for low pressure operation is, however, readily obtained by adopting a gauge structure of the Penning type.[3]

Here the cathode consists of two parallel plates connected electrically, and the anode is in the form of a circular wire placed midway between the plates. In addition, a small permanent magnet is arranged to provide a field perpendicular to the cathode plates. Electrons originating at the cathode are prevented by the magnetic field from moving directly to the anode which they can reach only after numerous traversals of the space between the cathode plates. As a consequence of the vastly increased path, many ionizing collisions occur and a strong discharge is obtained even at low pressures.

[3] F. M. Penning, Physica 4, 71 (1937).

In normal operation as a conventional Penning gauge, the continuous discharge current is taken as a measure of pressure and in practice calibration curves can be obtained from about 10^{-5} to 10^{-2} mm Hg. Beyond this pressure, the current becomes too insensitive to pressure to permit useful readings to be taken.

By suitable choice of dimensions it is, however, possible to construct a Penning type structure which will operate as an alternating discharge gauge from several mm Hg down to 10^{-2} mm Hg. At this pressure, the relaxation oscillations cease, but now a pressure regime has been reached where normal Penning type operation with the continuous discharge becomes possible. Using both modes of operation in succession, the gauge thus covers a range from the millimeter region down to 10^{-5} mm Hg.

A gauge head covering this range, which was developed for upper atmosphere measurements, is shown in Fig. 7.

The cathode plates are in the form of two circular aluminum disks of 35 mm diam, held 20 mm apart by means of a glass spacer to which they are cemented with Araldite. The anode ring (25 mm diam) is made of 18 S.W.G. copper wire and is likewise cemented to the spacer as shown. A strip of aluminum foil, 18 mm wide, is placed round the outside of the spacer to act as an electrostatic shield held at anode potential.

The whole unit is then encased in a block of Araldite which provides mechanical strength and electrical insula-

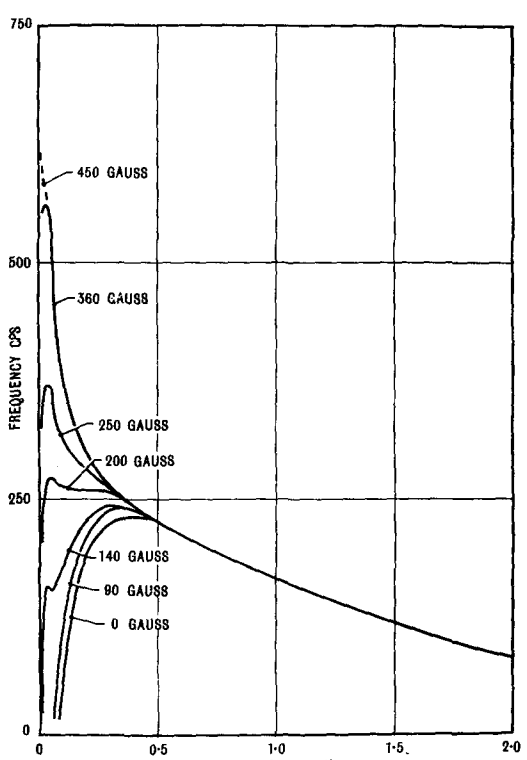

FIG. 9. Calibration curve of low pressure gauge for various values of magnetic field strength.

tion, and at the same time serves to anchor the inlet fitting by which the electrode assembly is attached to a mounting bracket together with the permanent magnet.

The pressure-firing-potential curves for a gauge of this type are shown in Fig. 8 for various values of magnetic field strength. The result of an increase in the field is a progressive lowering of the firing potential at low pressures, a feature which is desirable from the point of view of keeping the applied voltage required within reasonable limits. Towards higher pressures, however, the firing potential curves are all seen to converge and beyond about 0.5 mm Hg the influence of the field is quite negligible, at least over the range of field strength considered. At this pressure the mean free path has become sufficiently small for the directive effect of the field to be swamped by collisions of the electrons with gas molecules.

Figure 9 shows the calibration curve of the same gauge, again for several values of the magnetic field strength. In all cases, the operating voltage was 750 v and the parameters of the external circuit were $R=10$ megohms, $r=3000$ ohms, $C=1000\ \mu\mu f$.

Beyond 0.5 mm Hg, the calibration curves for all field strengths are seen to coincide, but on the low pressure side an increase in the field leads to the eventual development of a steep maximum and therefore to good pressure sensitivity of the gauge. Ultimately, at 450 gauss, the maximum is no longer reached and the continuous discharge sets in at a little below 10^{-2} mm Hg.

Beyond this point, normal Penning type operation is possible, for which the calibration curve is shown in Fig. 10. To ensure reliable striking of the discharge at low pressures it is however necessary to use an applied voltage of 1000 v. At the same time, this increase in voltage raises the high pressure limit of the instrument as an alternating

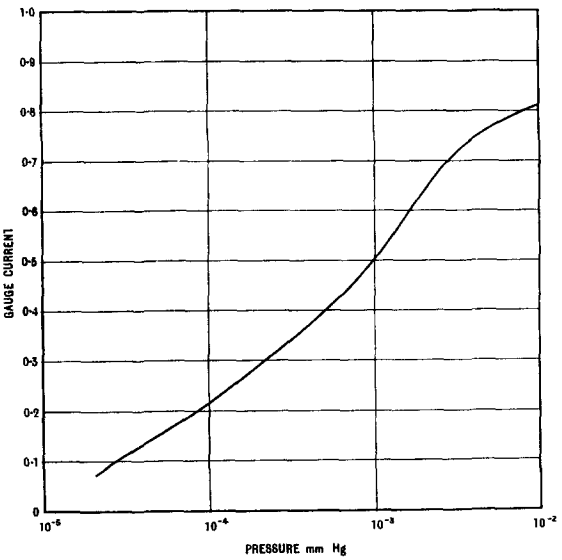

FIG. 10. Calibration curve of low pressure gauge for Penning mode of operation.

discharge gauge from 4 mm at 750 v to 6 mm at 1000 v so that the range covered by both modes of operation is from 6 mm Hg to 10^{-5} mm Hg.

As in the case of cylindrical gauges, the calibration curves showed good reproducibility and, at constant pressure, the frequency was stable within 1%.

ACKNOWLEDGMENTS

The author wishes to thank Dr. W. Schwietzke for his continued interest and encouragement. Publication is made with the permission of the Chief Scientist, Australian Defence Scientific Service, Department of Supply, Melbourne.

E.H. Hirsch (1964) Sputter-Ion Pumps With Thermionic Electron Injection.
Journal of Scientific Instruments, v. 41 (7), pp. 426-430, July 1964

E.H. Hirsch and I.K. Varga (1974) Thermionic Emission of Positive-Ions from Alkali Tantalates.
Journal of Physics D: Applied Physics, v. 7 (17), 2355-2361, November 1974

Ion emission from a dispenser source with sodium silicate matrix

E. H. Hirsch and I. K. Varga

Australian Defence Scientific Service, Department of Supply, Weapons Research Establishment, Salisbury, South Australia

(Received 8 April 1974; and in final form, 6 May 1974)

The increasing use of ion beam techniques in semiconductor technology has heightened interest in the development of new or improved ion sources, particularly those suitable for the generation of metal ions. Here surface ionization sources hold out promise, since they can meet the demands for both beam purity and compatibility with a high vacuum environment. Such sources, using ionizing surfaces of iridium[1,2] or oxygenated tungsten[3] have been successfully used to produce ions from materials with ionization potentials of up to about 6 eV. This requires operating the ionizer at about 1700°C, and since provision must also be made for generating a neutral atomic beam, the apparatus is relatively complex.

Great simplification would be achieved, if the material to be ionized could be dispersed in a suitable semiconducting matrix. Not only would this avoid the need for a neutral beam source, but, provided the semiconductor had a sufficiently high work function, it could be operated at a lower temperature, and the range of ionizable materials could be extended to those of higher ionization potential.

Based on such considerations, Zarabi and Satyam[4] have described a simple dispenser source, using as the matrix material sodium silicate, to which the desired metal is added as a small admixture, either in metallic powder form, or as an oxide. With sources of this type, they report to have obtained useful currents of Al^+, Sn^+, and Pb^+. The operating temperature is not stated but it is clear from the context that the emitters must have been run below the softening point of Pyrex, which limits the temperature to about 750°C. At this low temperature, the efficient surface ionization of materials with ionization potentials V_i exceeding 7 eV, such as Sn and Pb, would imply a very high emitter work function.

Under these conditions, alkali metal atoms from the silicate, which have a much lower ioization potential, could also undergo surface ionization, and could constitute a substantial portion of the total emission current. Unfortunately the measurements of Zarabi and Satyam were made in a simple diode system, which permitted only the total emission current, but not the ion species present, to be determined. The present work was therefore undertaken to determine mass spectrometrically the nature of the emitted ions.

Following Zarabi and Satyam, emitter material for Al^+ ions was prepared by adding 4% by weight of fine Al powder to sodium silicate, and producing a uniform mixture by grinding in isopropyl alcohol as a vehicle. When the alcohol had evaporated, a paste of suitable consistency was prepared by adding distilled water, after which the material was placed in the gap between a tantalum heater ribbon and a strip of fine molybdenum mesh, spot welded to the latter as shown in Fig. 1(a). The whole emitter was then briefly heated in air to about 120°C to remove moisture, prior to being mounted in the magnetic mass spectrometer shown schematically in Fig. 1(b).

Typical mass spectra obtained with this arrangement are shown in Fig. 2. These indicate only the presence of K^+

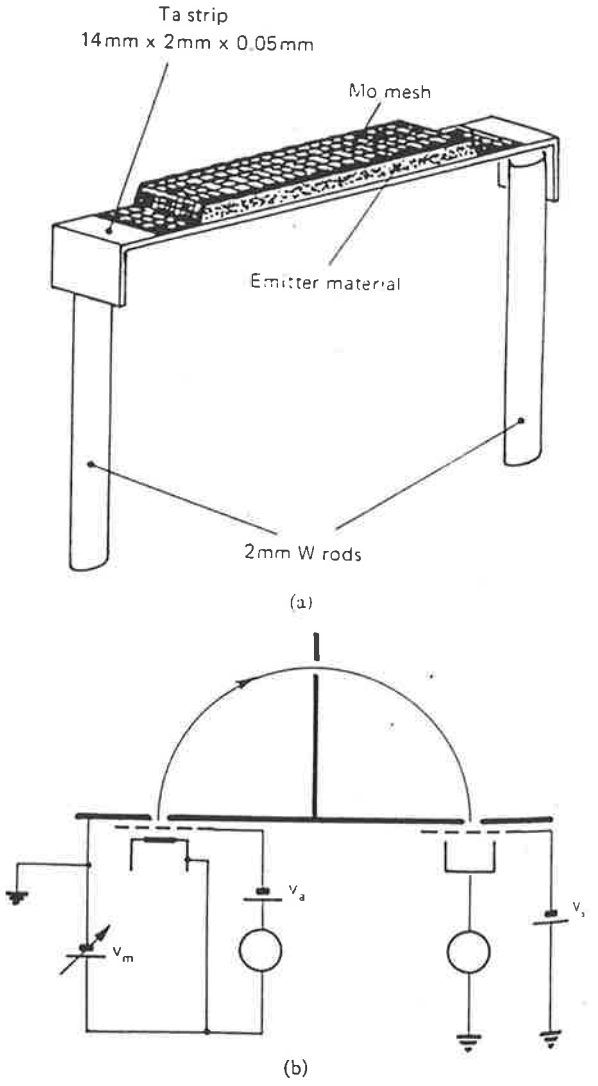

FIG. 1(a). Construction of emitter. (b) Mass spectrometer arrangement: V_a—ion accelerating potential; V_m—mass scanning potential; V_s—secondary electron suppression potential.

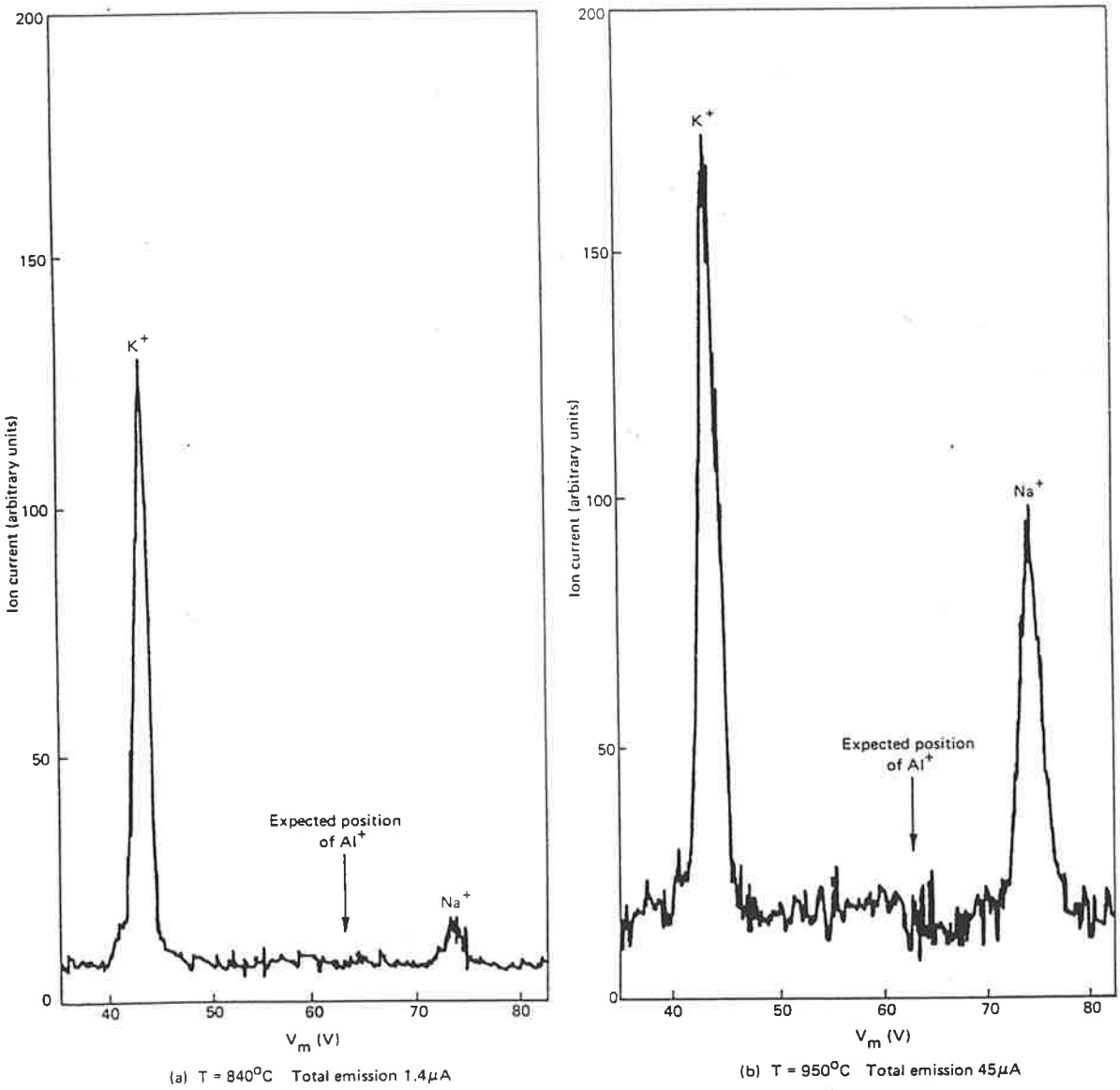

FIG. 2. Typical mass spectra. Arrow indicates expected position of Al^+.

and Na^+ ions, which originate from the matrix material, and there is no evidence at all of Al^+, the expected position of which in the spectrum is marked by arrows. Although potassium is present in the silicate only as a small impurity compared with the far more abundant sodium, the K^+ line is seen to be predominant, particularly at lower temperatures [Fig. 2(a)]. This is due to the fact that the ionization potential of K (4.34 eV) is considerably lower than that of Na (5.14 eV). However, as the Langmuir–Saha theory[5] predicts, the ratio of Na^+ to K^+ increases as the emitter temperature is raised [see Fig. 2(b)].

The temperature in Fig. 2(b) considerably exceeded that used by Zarabi and Satyam, but since even at this high temperature no Al^+ ions, having an ionization potential of 5.98 eV, could be detected, the surface ionization of Sn or Pb ($V_i = 7.33$ eV and 7.42 eV, respectively) would be quite impossible. It must therefore be concluded that the emission currents observed by Zarabi and Satyam were entirely due to alkali metal ions from the silicate, and that this material is not suitable as a dispenser matrix for metals of higher ionization potential.

[1]D. M. Jamba, Rev. Sci. Instrum. 40, 1072 (1969).
[2]R. G. Wilson, J. Appl. Phys. 44, 2130 (1973).
[3]H. L. Daley, J. Perel, and R. H. Vernon, Rev. Sci. Instrum. 37, 437 (1966).
[4]M. J. Zarabi and M. Satyam, Rev. Sci. Instrum. 42, 257 (1971).
[5]I. Langmuir and K. H. Kindgon, Phys. Rev. 34, 129 (1929).

E.H. Hirsch and J. Richards (1974) Pressure fluctuations in a diffusion pump using polyphenyl ether.
Vacuum, v. 24 (3), pp. 123–124, March 1974

E.H. Hirsch and T.J. McKay (1992) A comparison of perfluoropolyether and silicone diffusion pump fluids.
Vacuum, v. 43 (4), pp. 301–304, April 1992

E.H. Hirsch and T.J. McKay (1993) Emission and re-absorption of diffusion pump fluid breakdown products.
Vacuum, v. 44 (1), pp. 47–50, January 1993